

Stellar Oscillations in Modified Gravity

Jeremy Sakstein^{1,*}

¹*Department of Applied Mathematics and Theoretical Physics,
Centre for Mathematical Sciences, Cambridge CB3 0WA, United Kingdom*

Starting from the equations of modified gravity hydrodynamics, we derive the equations of motion governing linear, adiabatic, radial perturbations of stars in scalar-tensor theories. There are two new features: first, the eigenvalue equation for the period of stellar oscillations is modified such that the eigenfrequencies are always larger than predicted by General Relativity. Second, the General Relativity condition for stellar instability is altered so that the adiabatic index can fall below $4/3$ before unstable modes appear. Stars are more stable in modified gravity theories. Specialising to the case of chameleon-like theories, we investigate these effects numerically using both polytropic Lane-Emden stars and models coming from modified gravity stellar structure simulations. We find that the change in the oscillation period of Cepheid star models can be as large as 30% for order-one matter couplings and the change in the inferred distance using the period-luminosity relation can be up to three times larger than if one had only considered the modified equilibrium structure. We discuss the implications of these results for recent and up-coming astrophysical tests and estimate that previous methods can produce new constraints such that the modifications are screened in regions of Newtonian potential of $\mathcal{O}(10^{-8})$.

I. INTRODUCTION

Modified theories of gravity (MG) have received a lot of attention in the last decade. Upcoming surveys such as Euclid [1] and LSST [2] will test Einstein's theory of General Relativity (GR) on cosmological scales to incredibly high precision. On the theoretical side, the cosmological constant problem is driving the study of alternate theories of gravity in an attempt to explain why the observed vacuum energy density is 120 orders of magnitude smaller than the quantum field theory prediction (see [3] for a review). Cosmology probes the long-range, infra-red (IR) behaviour of gravity and so the majority of these theories are IR modifications, often involving new scalar-degrees of freedom which either drive the acceleration, screen out the effects of the cosmological constant or include some symmetry such that its value is technically natural. GR is the unique Lorentz-invariant theory of a massless spin-2 particle [4] and so any modification of GR necessarily introduces at least one new degree of freedom. These could be decoupled from matter, however, in any generic theory there is no symmetry forbidding this and so any decoupling is unnatural. If a coupling is present then one must face the issues of additional or *fifth*-forces that result whenever a field-gradient is present. GR has been tested to incredibly high precision over the last century and so one must fine-tune the strength of these couplings to incredibly small values in order to have a viable theory. Such small couplings usually render any modifications insignificant in all but the strongest gravitational fields. For example, any quintessence model of dark energy requires a mass for the scalar to be of order H_0 [5] so that the force-range is of the order of the observable universe. If such a field is then coupled to matter it must pass

laboratory tests, which require the force to be sub-mm [6]. Therefore, the only way to have a light quintessence-scalar coupled to matter is to tune all of the couplings to very small values. In general, there is no symmetry protecting these values and so quantum corrections are expected to induce order-one corrections. The small value of these couplings is therefore tantamount to fine-tuning.

There is one caveat to the above argument: all of the tests of GR have been performed in our local neighbourhood and so there is nothing preventing a theory which has large fifth-forces active over cosmological scales provided that these are somehow absent locally. Such theories are said to possess *screening mechanisms* and there are several examples in the literature including the chameleon mechanism [7, 8], the symmetron mechanism [9], the environment-dependent Damour-Polyakov effect [10], the Vainshtein mechanism [11] (see also [12–14] for applications to modern theories such as Galileons and massive gravity) and the disformal mechanism [15]. Most of the theories that include a screening mechanism have the property that the field-profile of the new degrees of freedom are sourced by the ambient density. They are constructed such that at high densities either the field's masses are large enough that the force is short-ranged, the effective coupling to matter becomes negligible or the field-gradients are suppressed with respect to the gradient of the Newtonian potential. The exception is the disformal mechanism where field gradients are sourced by pressure, which is generally negligible for non-relativistic sources and so no field-gradient is induced.

The problem is then changed from reconciling fifth-forces with local experiments to distinguishing these theories from GR observationally. Theories such as Galileons show interesting effects cosmologically through either the modified background expansion rate, linear perturbation properties or halo clustering effects [16–18], however, the same is not true of chameleons and symmetrons, where the cosmological mass of the field is al-

* j.a.sakstein@damtp.cam.ac.uk

ways less than 0.1Mpc^{-1} [19, 20], precluding any effects on linear scales. On non-linear scales, there can still be some galaxy clustering effects (see, for example [21–24] and references therein). Astrophysical tests of these theories can probe regions of parameter space where all cosmological signatures vanish and therefore have the potential to constrain them by several orders of magnitude below what is possible with cosmological tests.

Several astrophysical tests of different modified gravity theories have been investigated, including stellar-structure tests [25–27], black hole tests [28] and galactic dynamics tests [29–31]. Here, we will be concerned only with stellar structure. The purpose of this work is to present and investigate a consistent framework for dealing with the equations of modified gravity scalar fields coupled to hydrodynamics at zeroth- and first-order in perturbation theory with an aim to looking at both current and new observational tests. The effects of disformally coupled scalars on the equilibrium structure of non-relativistic stars are still unknown and a calculation is beyond the scope of this work. We hence focus on theories where the field is coupled to the trace of the energy momentum tensor only and the fifth-force is proportional to the field gradient and the strength of the matter coupling. This includes chameleon-like and Vainshtein screened theories. Starting from the modified equations of hydrodynamics, we derive the equations governing the equilibrium structure of stars (the modified stellar-structure equations) and the evolution of linearised, radial, adiabatic perturbations of both the field and stellar structure. We find three new effects in modified gravity:

1. When the star is unscreened, the period of oscillation can be reduced by an $\mathcal{O}(1)$ amount. For Cepheid stars, which are good probes of MG [27], we find that the change in the period can result in differences from the GR inferred distance measurement of up to three times what has been previously been calculated using an approximation and therefore that current bounds can be improved using the same data sets.
2. When the star is unscreened, the star is more stable to these perturbations. There is a well-known result in stellar astrophysics that when the adiabatic index falls below $4/3$ the squared-frequency of the fundamental mode is negative and so there is an unstable mode. We will show that in MG the index can fall below $4/3$ without any instability. In MG, there is no universal bound on the critical index for the appearance of the instability; its precise value depends on the structure and composition of the star as well as how unscreened it is.
3. The perturbations of the star can source scalar radiation and vice versa.

The first two effects require the star to be unscreened while the third does not. Vainshtein-screened theories

are too efficient to leave any star unscreened and so it is only the third effect that may be used to probe this theory. In this work, we will only investigate the first two effects and so for this reason, we will only deal explicitly with chameleon-like theories, although we will present the general derivation and comment briefly on the application to Galileon-like theories.

Chameleon-like theories screen according to the local Newtonian potential; objects where this is lower than a universal model parameter (to be defined below) are unscreened whereas they are screened when the converse is true. One is then led to look for MG effects in the most under-dense regions of the universe. In terms of the Newtonian potential, these are dwarf galaxies. Dwarf galaxies located in clusters are screened by the Newtonian potential of their neighbours whilst isolated dwarf galaxies may show MG effects. Recently, MG N-body codes have been combined with SDSS data to produce a screening map of the nearby universe [32]. This has allowed dwarf galaxy tests of MG using current data to be performed for the first time [27, 31].

In unscreened dwarf galaxies located in cosmological voids, main- and post-main-sequence stars may become partially unscreened leading to strong fifth-forces in their outer layers. The equilibrium structure of stars in chameleon-like theories has been well studied [25, 26]. These stars must provide a stronger outward pressure gradient in order to combat these additional forces than they would had they been GR stars. The extra energy per unit time required to source this gradient comes from an increased rate of nuclear burning in the core. A star under the influence of MG is therefore more luminous, more compact and has a higher effective temperature than its GR doppelgänger. A modified version of the publicly available code MESA, which can simulate the structure and evolution of stars in these theories was presented in [26] and has become a powerful tool in the quantitative prediction of astrophysical effects. At the level of perturbations, Cepheid-variable stars pulsate at a higher frequency and so obey a different period-luminosity (P-L) relation to the GR one. Using a simple approximation to find the new period, [27] have used MESA models to place the strongest constraints in the literature to date. The MG frequencies can be numerically computed by solving the new equations coming from modified gravity hydrodynamics and one aim of this work is to compare the new MG predictions with this approximation. The others are to investigate the stability of stars in these theories as well as the implications for current and possible future astrophysical tests.

This paper is then organised as follows: in section II, we present the action for chameleon-like theories and outline some of the essential features. We then examine the screening mechanism and present the two model-independent parameters that can be used to fully specify the effects of MG on the structure and evolution of stars. We then give a brief introduction to astrophysical tests of modified gravity and outline the current constraints.

In section III we derive the equations of modified gravity hydrodynamics. At zeroth-order, these give the modified equations of stellar structure. At first-order, we derive the equations of motion describing the coupled linear, radial, adiabatic perturbations of both the field and radial displacements. In section IV we specialise to the case where the scalar-radiation is negligible and elucidate the properties of the new equation of motion for stellar perturbations. In section V we show how the criterion for the star to be stable to these perturbations is altered in and argue that stars are more stable in MG. In section VI, we present numerical results. First, we investigate Lane-Emden models of convective stars and calculate the new oscillation periods and critical value of the adiabatic index. We then turn our attention to MESA models. We calculate the change in the period and inferred distance from the P-L relation for the same Cepheid models used in [27] in order to assess the accuracy of their approximation and find that when the full effects of hydrodynamic perturbations are included, the differences from GR can be up to three times larger than the approximation predicts. Using this, we estimate the new constraints that can be found using the same data-sets and procedure as [27]. These correspond to constraints where the modifications are screened in regions of Newtonian potential $\Phi_n \sim \mathcal{O}(10^{-8})$. Finally, we discuss our results in light of recent and future astrophysical tests and conclude in section VII.

II. SCREENED SCALAR-TENSOR GRAVITY

A. The Action

Any theory which contains a scalar ϕ gravitationally-coupled to matter fields ψ_i will generically result in modifications of the Newtonian force-law in the non-relativistic limit and therefore constitute a modified theory of gravity. One well-studied class of model has this coupling arise because the metric $\tilde{g}_{\mu\nu}$ in the matter Lagrangian differs from the metric appearing in the Ricci scalar $g_{\mu\nu}$ by a conformal factor $A(\phi)$ such that

$$\tilde{g}_{\mu\nu} = A^2(\phi)g_{\mu\nu}. \quad (1)$$

Typically, $A(\phi) \approx 1 + \mathcal{O}(\phi/M_{\text{pl}})$ so that the theories do not differ too greatly between frames. These theories are described by the general action

$$S = \int d^4x \left[\frac{M_{\text{pl}}^2}{2} R - \frac{1}{2} \nabla_\mu \phi \nabla^\mu \phi - V(\phi) \right] \quad (2)$$

$$+ S_m[\psi_i; A^2(\phi)g_{\mu\nu}] \quad (3)$$

and give rise to a Newtonian fifth-force (per unit mass)

$$\vec{F}_\phi = \frac{\beta(\phi)}{M_{\text{pl}}} \nabla \phi, \quad \text{where} \quad \beta(\phi) \equiv M_{\text{pl}} \frac{d \ln A(\phi)}{d\phi} \quad (4)$$

is known as the *coupling*. Theories with screening mechanisms generally have the property that $d\beta(\phi)/d\phi \approx 0$ in

the unscreened region [33]. This form of the action is referred to as the *Einstein frame* action since the *Einstein frame metric*, $g_{\mu\nu}$, is used to compute the Ricci scalar and not the *Jordan frame metric* $\tilde{g}_{\mu\nu}$. One may instead work in the *Jordan Frame*, in which case the action can be obtained using the Weyl rescaling (1). In what follows we will work exclusively in the Einstein frame since it allows for intuitive physical interpretations of the new features of stellar structure and perturbation theory. A subset of these theories has received a lot of attention recently because certain choices of the scalar potential $V(\phi)$ and conformal factor $A(\phi)$ can lead to local screening of the fifth-force (4) through either the chameleon mechanism [7, 8], the symmetron mechanism [9] or the environment-dependent Damour-Polyakov effect [10]. In what follows, we will use a model-independent parametrisation of the theory parameters which is well-suited for astrophysical tests and refer the reader to [19, 26, 34–36] for the specific details of individual screening mechanisms.

Before going on to discuss the high-density screening mechanism, it is important to address the notion of a conserved matter density. The conformal coupling of the field to the visible sector has the result that the energy-momentum tensor of matter $T_m^{\mu\nu} = 2/\sqrt{-g}\delta S_m/\delta g_\nu$ is not covariantly conserved, rather one has $\nabla_\mu T_m^{\mu\nu} = \beta(\phi)T_m \nabla^\nu \phi/M_{\text{pl}}$, where T_m is the trace of the energy-momentum tensor. The density $\rho_m \equiv -T_m$ does not obey the usual continuity equation and one generally works with the conserved density $\rho_m \equiv A(\phi)\rho$ instead. This conserved density is also field-independent. From here on we shall refer to ρ as the conserved matter density corresponding, for example, to the stellar mass per unit volume.

B. The Screening Mechanism

The coupling to matter has the effect that the scalar potential appearing in the action (2) is not the same scalar potential which governs the field's dynamics. Instead, the equation of motion is

$$\square\phi = \frac{dV(\phi)}{d\phi} + \frac{\beta(\phi)\rho}{M_{\text{pl}}} \quad (5)$$

corresponding to a density-dependent effective potential

$$V_{\text{eff}}(\phi) = V(\phi) + \rho A(\phi). \quad (6)$$

It is this density-dependence which is responsible for screening the fifth-force in over-dense environments. Suppose that this potential has a minimum. The field-position of this minimum can differ by many orders of magnitude between the solar-system and the cosmological background (recall $\rho_\oplus/\rho_0 \sim 10^{29}$) and so it is possible to engineer effective potentials where either the mass of small oscillations about the high-density minimum is large such that the range of the fifth-force is sub- μm [8] or the coupling $\beta \ll 1$ and the magnitude of the force

is negligible [9, 10]. In this way, the fifth-force is undetectable in high-density areas.

One can then ask exactly when an object will be screened. Consider a spherically symmetric over-density with profile $\rho_b(r)$ and radius R , which is a small perturbation about a lower but more spatially-extensive constant density ρ_c whose characteristic length-scale is $\gg R$. For example, a galaxy in the cosmological background or a star inside a galaxy. If R is large enough such that the field can reach its minimum ϕ_b at the higher density and remain there over most of the object's interior then the fifth-force will be negligible and the object is screened. If the converse is true and the field deviates only from the value in the background ϕ_c by a small perturbation then the full effects of the modification of GR will manifest. In the static, non-relativistic limit we can ignore time-derivatives and so the equation of motion (5) is:

$$\nabla^2\phi = V_{,\phi} + \frac{\beta(\phi)\rho}{M_{\text{pl}}}. \quad (7)$$

There are then two cases to consider. First, if the field can reach its minimum we have $V_{,\phi} \approx -\beta\rho/M_{\text{pl}}$ and equation (7) is unsourced. In this case the field is just

constant and equal to the high-density minimum value so that $\phi(r) \approx \phi_b$. When this solution is valid, there are no fifth-forces but in general there is some radius r_s , known as the *screening radius*, where the field begins to move away from this value and we expect large fifth-forces in this region. In this second case, the field is a small perturbation about the under-dense value so that $\phi(r) = \phi_0 + \delta\phi(r)$. Subtracting the equation of motion in both the over and under-dense regions and linearising we have

$$\nabla^2\delta\phi \approx m_c^2\delta\phi + \frac{\beta_c\delta\rho}{M_{\text{pl}}}, \quad (8)$$

where $\delta\rho \equiv \rho_b - \rho_c$, $m_c^2 \equiv V_{,\phi\phi}(\phi_c)$ is the mass of the field in the background, $\beta_c \equiv \beta(\phi_c)$ and we have used the fact that $d\beta/d\phi \approx 0$. In all theories of interest, we have $m_c R \ll 1$ so that the fifth-force gives rise to novel features on large scales and so we have ignored the first term, it is negligible compared with the Laplacian. Now we know that $\delta\rho$ is related to the Newtonian potential Φ_N via the Poisson equation, $\nabla^2\Phi_N = 4\pi G\delta\rho$ and so we may substitute this into (8) and integrate twice to find the field profile:

$$\delta\phi(r) \approx -\phi_c + 2\beta_c M_{\text{pl}} \left[\Phi_N(r) - \Phi_N(r_s) + r_s^2 \Phi_N'(r_s) \left(\frac{1}{r} - \frac{1}{r_s} \right) \right] H(r - r_s), \quad (9)$$

where $H(x)$ is the Heaviside step-function. We refer to the region $r < r_s$ as the *screened* region and the region $r > r_s$ as *unscreened*. Using the definition of the Newtonian potential $d\Phi_N/dr = GM(r)/r^2$, where $M(r)$ is the mass enclosed within a sphere of radius r (the total mass of the over-density is $M = M(R)$), the fifth-force (4) in the unscreened region is given by the derivative of (9):

$$\frac{\beta_c}{M_{\text{pl}}} \frac{d\phi}{dr} = \alpha \frac{GM(r)}{r^2} \left[1 - \frac{M(r_s)}{M(r)} \right], \quad (10)$$

where $\alpha_c \equiv 2\beta^2(\phi_c)$. We will assume that there are no fifth-forces when $r < r_s$ and that the force is given by equation (10) when $r \geq r_s$ from here on [37]. When $r_s = R$ there is no fifth-force and the object is screened whereas when $r_s = 0$ the object is full unscreened and we have $F_\phi = \alpha_c F_N$, where F_N is the Newtonian force. The parameter α_c therefore determines the strength of the fifth-force.

All that remains is to find the screening radius r_s . Using the fact that $\delta\phi \rightarrow 0$ when $r/r_s \rightarrow \infty$ as does $\phi_N(r)$, equation (9) gives us an implicit expression for the screening radius:

$$\frac{\phi_c}{2\beta(\phi_c)M_{\text{pl}}} \equiv \chi_c = -\Phi_N(r_s) - r_s \Phi_N'(r_s) \geq 0. \quad (11)$$

It will be useful later to recast this as an integral equa-

tion:

$$\chi_c = 4\pi G \int_{r_s}^R r \rho_b(r) dr. \quad (12)$$

The parameter χ_c is known as the *self-screening parameter* and is of paramount importance to the screening properties of these theories. Since $\Phi_N < 0$ and $d\Phi_N/dr > 0$, there are no solutions when

$$|\Phi_N(R)| = \frac{GM}{R} > \chi_c. \quad (13)$$

In this case, the object is fully screened and $r_s = R$. When $\Phi_N > \chi_c$ the object will be at least partially unscreened.

The screening and fifth-force properties in any region are fully specified by α_c and χ_c , however these are very environment-dependent and are non-linearly related to the field values in different regions of the universe. The exception to this is unscreened objects, where the field is only a small perturbation around the value in the background and so these values are roughly constant. Astrophysical tests of MG [26, 27, 29, 31, 32] are performed by comparing the properties of screened and unscreened galaxies. Whether or not a galaxy is screened or not depends on its Newtonian potential relative to the cosmological value of χ_c ; the same is true of denser objects

in unscreened galaxies. In each case, the strength of the fifth-force in any unscreened region is proportional to the cosmological value of α_c and so astrophysical tests of MG probe the cosmological values of α_c and χ_c . The theory is then parametrised in a model-independent manner by the cosmological values of these parameters, which we denote by α , which measures the strength of the fifth-force in unscreened regions and χ_0 , which determines how small the Newtonian potential must be in order for the object to be unscreened [38]. We will work with this parametrisation in what follows. $f(R)$ theories are chameleon theories with $\alpha = 1/3$ [39] and χ_0 is equivalent to the derivative of the function today, f_{R0} .

C. Astrophysical Tests of Modified Gravity

We will not attempt any comparison with data here but for completeness and motivation we will describe the basic premise behind observational tests using astrophysical effects below.

1. Current Constraints

Only unscreened objects will show deviations from GR and so we must look for such objects in the universe if we wish to observe these deviations. There are two classes of screened objects: self-screened, where the self-Newtonian potential of the object is larger than χ_0 and environment-screened, where the object would be unscreened in isolation but is still screened due to the Newtonian potential of its neighbours (see [40] for a nice discussion of equivalence principle violation effects and their relation to environmental screening). The cosmological bound coming from cluster constraints is $\chi_0 \lesssim 10^{-5}$ [41]. The Newtonian potential of spiral galaxies is $\mathcal{O}(10^{-6})$ and so this would leave most galaxies, including our own milky way self-unscreened. Clearly if this were the case then our own galaxy would show deviations from GR, which are not observed and so we must conclude that our own galaxy is screened, either because $\chi_0 \lesssim 10^{-6}$ or because we are screened by the Newtonian potential of the local group. While this has been debated in the past, recently, an independent constraint from comparing water maser distances to NGC 4258 with tip of the red giant branch distances has placed the bound $\chi_0 < 10^{-6}$ [27]. Finally, the strongest constraints on χ_0 come from comparing tip of the red giant branch distances with Cepheid distances and place the bound $\chi_0 \lesssim 4 \times 10^{-7}$ [27].

2. Dwarf Galaxy Tests

With this bound, there are very few unscreened objects in the universe. There are no cosmological signatures, either at the level of the background or linear perturbations (although see [42, 43] for an unusual model with a

very strong coupling to matter) and spiral galaxies are screened. The only self-unscreened objects in the universe are dwarf galaxies, whose Newtonian potentials are $\mathcal{O}(10^{-8})$ and large post-main-sequence stars [44]. Isolated dwarf galaxies located in voids should therefore show deviations from GR compared to their counterparts located in clusters. The basic premise then is to compare the observational properties altered by MG in a sample of screened and unscreened dwarf galaxies. Any statistically significant discrepancy is a sign of MG whereas an agreement within experimental errors constrains χ_0 and α . One then needs some method of discerning whether or not an observed galaxy is screened. Recently, the results of MG N-body simulations have been used in conjunction with Sloan Digital Sky Survey (SDSS) data to provide a screening map of the universe for different values of χ_0 [32]. Using this map, it has already been possible to place new constraints on these theories [27, 31].

Observational signatures using dwarf galaxies generally fall into two classes: modifications of the galaxy dynamics [29] and those resulting from effects on stellar structure [25, 26]. Both have been carried out [27, 31] using SDSS data and, currently, the former is not competitive with the latter. In this work we are interested in stellar structure effects and so we shall only describe these here.

The most practical method for using stellar structure tests is to compare different distance indicators to the same galaxy. The distance to a galaxy using stellar phenomena is either calibrated on Milky Way (or local group galaxies in some cases) objects or derived from the GR theoretical model. Either way, if the stellar property used to calculate this distance is altered in MG then the measured distance to an unscreened galaxy will differ from the GR distance. If, on the other hand, the indicator is insensitive to MG then any observation will give precisely the GR distance. If one then compared two distances to the same galaxy, one using a screened distance indicator and the other using an unscreened one, any discrepancy probes MG. By using many different galaxies and comparing to a screened sample, a statistically significant constraint can be achieved. This is what was done in [27].

3. Cepheid Distances in Modified Gravity

In practice, the best unscreened distance indicators are Cepheid variable stars. They have Newtonian potentials of $\mathcal{O}(10^{-7}) - \mathcal{O}(10^{-8})$ and there is a large amount of data available.

Cepheid stars are 5-10 M_\odot stars which have evolved off the main-sequence and onto the red giant branch. During this phase, their Hertzsprung-Russell (HR) diagrams show a so-called blue loop, where the temperature rapidly increases and decreases at approximately constant luminosity. Whilst traversing the loop, the tracks cross the *instability strip*, where the star is unstable to *Cepheid*

pulsations. Along this narrow strip in the $\log L$ - $\log T_{\text{eff}}$ plane, the star is unstable due to a layer of partially ionised helium coinciding with the region where the motion becomes non-adiabatic. Upon compression, the energy does not go into raising the pressure, which would result in an increased outward force giving a stabilising effect but rather into further ionising the helium. This damming up of the energy acts like an engine and drives large changes, up to 10%, in the stellar radius. Along this strip, there is a well-known period luminosity relation:

$$M_{\text{B}} = a \log \tau + b \log(B - V) + c, \quad (14)$$

where M_{B} is the bolometric magnitude and a , b , and c are empirically determined constants. Empirically, $a \approx -3$ [45]. Now in MG, and we will see this derived below, the period τ of a Cepheid at fixed luminosity, effective temperature and mass change by some amount $\Delta\tau = \tau_{\text{MG}} - \tau_{\text{GR}}$ so that this empirically-fitted relation predicts a deviation from the GR distance

$$\frac{\Delta d}{d} = -\frac{1}{2}a \frac{\Delta\tau}{\tau}. \quad (15)$$

Previously [27], $\Delta\tau$ was calculated using the approximation $\Delta\tau/\tau \approx -\Delta G/2G$, where ΔG is calculated using some appropriate average. In this work, we will derive the equations governing its value and show how it can be calculated numerically using some simple examples and compare our results with this approximation.

III. MODIFIED GRAVITY HYDRODYNAMICS

In this section we shall start from the modified equations of hydrodynamics and proceed to derive the equations governing both the equilibrium structure and linearised radial perturbations of non-relativistic stars.

We will describe bulk quantities such as the pressure and density in the *Eulerian picture*, where these quantities are to be considered as fields which give the value of said quantities at any point in space as a function of time. In contrast, we will describe the position of individual fluid elements (and, when needed, the pressure perturbations) in the *Lagrangian picture*, where the motion of individual fluid elements are followed as a function of time. In this case, the Lagrangian position \vec{r} of a fluid element satisfies the momentum equation:

$$\frac{\partial^2 \vec{r}}{\partial t^2} = -\frac{1}{\rho} \nabla P + \vec{F}, \quad (16)$$

where $P(\vec{r})$ is the pressure, $\rho(\vec{r})$ is the density and \vec{F} is the external force density. In MG, the fluid moves under its own Newtonian gravity and the fifth-force (4) due to the scalar field so that

$$\frac{\partial^2 \vec{r}}{\partial t^2} = -\frac{1}{\rho} \nabla P - \frac{GM(r)}{r^3} \vec{r} - \frac{\beta(\phi)}{M_{\text{pl}}} \nabla \phi. \quad (17)$$

This is the only hydrodynamical equation that is altered relative to GR; changing gravity only changes the motion of the fluid elements and does not directly[46] alter other processes such as mass conservation, energy generation and radiation flux. The quantity $M(r)$ ($r \equiv |\vec{r}|$) is the mass enclosed inside a radius r from the centre, and is given via the Poisson equation

$$\nabla^2 \Phi_{\text{N}} = 4\pi G \rho(r), \quad (18)$$

which may be integrated once to give

$$\frac{d\Phi_{\text{N}}}{dr} = \frac{GM(r)}{r^2}. \quad (19)$$

Since mass is a locally-conserved quantity we also have the continuity equation:

$$\frac{\partial \rho}{\partial t} + \vec{\nabla} \cdot (\rho \vec{v}) = 0, \quad (20)$$

where $\vec{v} \equiv d\vec{r}/dt$ is the velocity of the fluid element. In general, one must also consider the energy generation and radiative transfer equations but these are only important if one wishes to study the effects of perturbations coupled to stellar atmospheres, which is irrelevant in the context of modified gravity. We will include their effects when simulating the equilibrium stellar configuration numerically in order to produce the correct stellar properties, however, we will not include them in our perturbation analysis. Instead, we will work in the so-called *adiabatic* approximation, where the density and pressure evolve according to

$$\frac{dP}{dt} = \frac{\Gamma_1 P}{\rho} \frac{d\rho}{dt}. \quad (21)$$

The quantity

$$\Gamma_1 \equiv \left(\frac{d \ln P}{d \ln \rho} \right)_{\text{adiabatic}} \quad (22)$$

is the *first adiabatic index* or *equation of state*. It is of paramount importance to the study of stellar pulsation and stability and we will return to discuss it later on. The simplest gases are typically characterised by a constant equation of state so that $P \propto \rho^{\Gamma_1}$, where $\Gamma_1 = 5/3$ ($4/3$) for non-relativistic (relativistic) gases. In general, one must couple the hydrodynamic equations to the full radiative transfer system and extract the equation of state from the result.

A. Equilibrium Structure

We are interested in small perturbations about the equilibrium structure of stars and so we must first find the modified zeroth-order equations. These were presented heuristically in [26], however, here we shall derive them from this more formal set-up. The equilibrium stellar configuration is both static and spherically symmetric

and can be found by setting time-derivatives to zero and $\vec{r} = r$ in the hydrodynamic equations so that this now represents the Eulerian coordinate. We will denote all equilibrium quantities with a subscript-zero except for $M(r)$, which is defined at the background level only. It is important to note that χ_0 is not a property of the star but is the cosmological value of χ_c found by evaluating (11) using the cosmological values of ϕ and β . In what follows, $\phi_0(r)$ is the equilibrium field-profile throughout the star and not the cosmological value. With no time-dependence, (20) is trivially satisfied and $\rho(r, t) = \rho(r)$. This simple form of the density profile allows us to find the mass enclosed in any given radius:

$$\frac{dM(r)}{dr} = 4\pi r^2 \rho_0(r). \quad (23)$$

The momentum equation (17) then reduces to the *modified hydrostatic equilibrium equation*

$$\frac{dP_0(r)}{dr} = -\frac{GM(r)\rho_0(r)}{r^2} - \frac{\beta(\phi_0)\rho_0(r)}{M_{\text{pl}}} \frac{d\phi_0(r)}{dr}. \quad (24)$$

Physically, this equation describes the pressure profile the star must assume in order for the star to support itself against gravitational collapse. The second term is the fifth-force due to the scalar field; stars in modified gravity need to provide larger pressure gradients in order to combat this extra inward component [25–27]. These equations are then supplemented by the radiative transfer equation

$$\frac{dT_0(r)}{dr} = -\frac{3}{4a} \frac{\kappa(r)}{T_0^3} \frac{\rho_0(r)L_0(r)}{4\pi r^2}, \quad (25)$$

which describes how the temperature $T(r)$ varies due to the flux of energy with luminosity $L(r)$ away from regions of energy generation governed by

$$\frac{dL_0}{dr} = 4\pi r^2 \rho_0(r) \epsilon(r). \quad (26)$$

Here, $\kappa(r)$ is the *opacity*, the cross-section for radiation absorption per unit mass and $\epsilon(r)$ is the energy generation rate per unit mass from processes such as nuclear burning.

Taken by themselves, these equations do not close and one must specify the equations of state relating P_0 , ρ_0 , κ and ϵ , which are themselves determined by further equations involving energy transfer and nuclear burning networks. In the subsequent sections, we will solve these equations analytically by assuming different equations of state. When computing the equilibrium structure using MESA, look-up tables are used to find the opacity and pressure at a given density and temperature while energy generation rates are found using nuclear burning networks for individual elements. We refer to reader to the MESA instrumentation papers [47, 48] for the full details.

B. Linear Perturbations

The dynamics of stellar oscillations are governed by the hydrodynamics of small perturbations about the equilibrium configuration and so we shall linearise the equations (17), (18), (20) about some assumed background profile $\{P_0(r), \rho_0(r), \Phi_{\text{N},0}(r), \Gamma_{1,0}(r), \phi_0(r)\}$ ignoring second-order terms in the perturbations.

The fundamental object of interest is the linearised perturbation to the Lagrangian position of each fluid element $\vec{\delta r}(\vec{r})$, which describes the oscillation of the fluid from equilibrium at each radius. So far, our treatment has been completely general and we have worked with the full three-dimensional problem. Continuing in this fashion would result in a complete treatment of both radial and non-radial modes of oscillation. The aim of this work is to provide a consistent framework with which to predict the oscillation properties of partially unscreened stars residing in unscreened dwarf galaxies. The extragalactic nature of these stars ensures that only their fundamental radial mode (and possibly the first-overtone) are observable and so from here on we will specify to the case of radial oscillations so that $\vec{\delta r}(r)$ is a purely radial vector[49]. A more convenient quantity to work with is the relative displacement, given by

$$\zeta(r) \equiv \frac{\delta r(r)}{r}, \quad (27)$$

and the goal of the present section is to derive is equation of motion.

We shall work with Eulerian perturbations of the background profile, which we will distinguish from Lagrangian perturbations by the use of a tilde so that

$$P(r, t) = P_0(r) + \tilde{P}(r, t) \quad (28)$$

$$\rho(r, t) = \rho_0(r) + \tilde{\rho}(r, t) \quad (29)$$

$$\Phi_{\text{N}}(r) = \Phi_{\text{N},0}(r) + \tilde{\Phi}_{\text{N}}(r, t) \quad (30)$$

$$\phi(r, t) = \phi_0(r) + \tilde{\phi}(r, t). \quad (31)$$

As remarked above, the Lagrangian perturbations may provide more physical insight on occasion and the two are related, for example, via

$$\delta P(r, t) = P(\vec{r} + \vec{\delta r}, t) - P_0(r) \quad (32)$$

$$= \tilde{P}(r, t) + \delta r \frac{dP_0(r)}{dr}. \quad (33)$$

It will be useful later to have the Lagrangian pressure perturbation in terms of our system-variables. This is given by

$$\frac{\delta P}{P_0} = \Gamma_{1,0} \frac{\delta \rho}{\rho_0} = -\Gamma_{1,0} \left(3\zeta + r \frac{d\zeta}{dr} \right), \quad (34)$$

where the first equality holds only in the adiabatic approximation.

We begin by perturbing equation (20) to find

$$\tilde{\rho} = -\frac{1}{r^2} \frac{\partial}{\partial r} (r^3 \rho_0 \zeta). \quad (35)$$

This may be used in the perturbed form of (17) to find[50]

$$\rho_0 r \frac{\partial^2 \zeta}{\partial t^2} = -\frac{d\tilde{P}}{dr} - \rho_0 \frac{d\tilde{\Phi}_N}{dr} + \frac{\beta_0}{M_{\text{pl}} r^2} \frac{\partial}{\partial r} (r^3 \rho_0 \zeta) \frac{d\phi_0}{dr} - \frac{\beta_0 \rho_0}{M_{\text{pl}}} \frac{d\tilde{\phi}}{dr}. \quad (36)$$

The perturbed Poisson equation is

$$\nabla^2 \tilde{\Phi}_N = 4\pi G \tilde{\rho}, \quad (37)$$

which may be integrated once using (35) to find

$$\frac{d\tilde{\Phi}_N}{dr} = -4\pi G r \rho_0 \zeta. \quad (38)$$

Now

$$\frac{dP}{dt} = \frac{\partial P}{\partial t} + \vec{v} \cdot \nabla P = \frac{\partial \tilde{P}}{\partial t} + r \frac{\partial \zeta}{\partial t} \frac{\partial P_0}{\partial r} \quad (39)$$

and using (21) this is

$$\tilde{P} + r \zeta \frac{\partial P_0}{\partial r} = \frac{\Gamma_{1,0} P_0}{\rho_0} \left(\tilde{\rho} + r \zeta \frac{\partial \rho_0}{\partial r} \right). \quad (40)$$

We wish to eliminate \tilde{P} and $\tilde{\rho}$ and so we substitute (35) into (40) to find

$$\tilde{P} = -\frac{\Gamma_{1,0} P_0}{\rho_0} \left(\frac{1}{r^2} \frac{\partial}{\partial r} (r^3 \rho_0 \zeta) - r \zeta \frac{dP_0}{dr} + \frac{\rho_0}{\Gamma_{1,0} P_0} \frac{dP_0}{dr} r \zeta \right)$$

$$= -\Gamma_{1,0} P_0 r \left(\frac{\partial \zeta}{\partial r} + \frac{3}{r} \zeta + \frac{1}{\Gamma_{1,0} P_0} \frac{dP_0}{dr} \zeta \right). \quad (41)$$

We then have

$$\begin{aligned} \frac{\partial \tilde{P}}{dr} &= -\frac{\partial}{\partial r} (\Gamma_{1,0} r P_0 \frac{\partial \zeta}{\partial r}) \\ &\quad - \frac{\partial}{\partial r} (3\Gamma_{1,0} P_0 \zeta) - \frac{\partial}{\partial r} (r \frac{dP_0}{dr} \zeta). \end{aligned} \quad (42)$$

This may then be used with (37) and (36) to find:

$$\begin{aligned} r^4 \rho_0 \frac{\partial^2 \zeta}{\partial t^2} &= \frac{\partial}{\partial r} \left(r^4 \Gamma_{1,0} P_0 \frac{\partial \zeta}{\partial r} \right) + r^3 \frac{\partial}{\partial r} [(3\Gamma_{1,0} - 4) P_0] \zeta \\ &\quad - \frac{r^3 \beta_0 \rho_0}{M_{\text{pl}}} \frac{\partial \tilde{\phi}}{\partial r} - \frac{\beta_0 \rho_0}{M_{\text{pl}}} r^4 \frac{d^2 \phi_0}{dr^2} \zeta - 2 \frac{r^3 \beta_0 \rho_0}{M_{\text{pl}}} \frac{d\phi_0}{dr} \zeta. \end{aligned} \quad (43)$$

This is the equation of motion governing the evolution of ζ . In GR, $\partial \tilde{\phi} / \partial r = 0$ and we obtain a single equation. In MG, however, we need a separate equation for $\tilde{\phi}$, which is found by perturbing the equation of motion (5):

$$-\frac{\partial^2 \tilde{\phi}}{\partial t^2} + \nabla^2 \tilde{\phi} = m_0^2 \tilde{\phi} - 3 \frac{\beta}{M_{\text{pl}}} \rho_0 \zeta - \frac{\beta}{M_{\text{pl}}} r \frac{\partial}{\partial r} (\rho_0 \zeta), \quad (44)$$

where $m_0^2 \equiv V_{\phi\phi}(\phi_0)$ is the mass of the unperturbed field at zero density and equation (35) has been used. We are interested in stationary-wave solutions and so we expand

$$\zeta(r, t) = \xi(r) e^{i\omega t} \quad (45)$$

$$\tilde{\phi}(r, t) = \varphi(r) e^{i\omega t} \quad (46)$$

to yield two coupled equations

$$(\nabla^2 + \omega^2) \varphi = m_0^2 \varphi - 3 \frac{\beta}{M_{\text{pl}}} \rho_0 \xi - \frac{\beta}{M_{\text{pl}}} r \frac{\partial}{\partial r} (\rho_0 \xi), \quad (47)$$

$$\frac{d}{dr} \left(r^4 \Gamma_{1,0} P_0 \frac{d\xi}{dr} \right) + r^3 \frac{d}{dr} [(3\Gamma_{1,0} - 4) P_0] \xi - \frac{r^4 \beta_0 \rho_0}{M_{\text{pl}}} \frac{d^2 \phi_0}{dr^2} \xi - 2 \frac{r^3 \beta_0 \rho_0}{M_{\text{pl}}} \frac{d\phi_0}{dr} \xi + r^4 \rho_0 \omega^2 \xi = \frac{r^3 \beta_0 \rho_0}{M_{\text{pl}}} \frac{d\varphi}{dr}. \quad (48)$$

Equations (47) and (48) constitute the main result of this section. One could combine them into a single equation, however, it is more instructive to treat the system as two coupled equations. In GR, we have $\varphi = \beta_0 = d\phi_0/dr = 0$ and (48) reduces to

$$\begin{aligned} \frac{d}{dr} \left(r^4 \Gamma_{1,0} P_0 \frac{d\xi}{dr} \right) \\ + r^3 \frac{d}{dr} [(3\Gamma_{1,0} - 4) P_0] \xi + r^4 \rho_0 \omega^2 \xi = 0, \end{aligned} \quad (49)$$

which describes linear, adiabatic, radial waves moving in the stellar interior. It is known at the *linear adiabatic*

wave equation (LAWE) and its eigenfrequencies ω give the frequency of stellar oscillations about equilibrium. We will hence refer to (48) as the *modified linear adiabatic wave equation* (MLAW). Its properties will be the subject of the next section.

Using the profile (10), we have

$$\frac{\beta_0}{M_{\text{pl}}} \left[2 \frac{d\phi_0}{dr} + r \frac{d^2 \phi_0}{dr^2} \right] = 4\pi \alpha G r \rho_0(r) \quad r > r_s, \quad (50)$$

which we shall use in all analytic and numerical computations from here on.

C. Application to Other Modified Gravity Theories

Before proceeding, it is worth noting that although this work focuses on chameleon-like theories, the hydrodynamic analysis performed so far is more general than this. Any scalar-tensor theory whose Einstein frame matter coupling can be written in the effective form

$$\mathcal{L}_{\text{coupling}} = C(\phi)T_{\text{m}}, \quad (51)$$

where T_{m} is the trace of the matter energy-momentum tensor, will give rise to an additional force

$$\vec{F}_{\phi} = \frac{\beta(\phi)}{M_{\text{pl}}} \nabla \phi \quad \beta(\phi) \equiv M_{\text{pl}} \frac{dC(\phi)}{d\phi}, \quad (52)$$

provided that ϕ is the canonically normalised field [51]. The only assumption we have made so far is $d\beta(\phi)/d\phi \approx 0$ but this was not necessary, only appropriate, and if one has a scalar-tensor theory where this is not the case then one would find additional terms in (48). In terms of the theories studied so far we have $C(\phi) = \ln A(\phi)$. Another class of theories that has attracted recent interest are those which screen via the Vainshtein mechanism [11] such as Galileons [12] and massive gravity [14, 52], which are described by $C(\phi) = \gamma\phi/M_{\text{pl}}$ where γ is a constant describing the strength of the fifth-force. In this case, one has $\beta(\phi) = \gamma$ so that $d\beta/d\phi = 0$. The MLawe (48) therefore applies equally to Vainshtein screened theories provided that one provides the counterpart to the equation of motion for the field perturbation (47). Vainshtein screening is too efficient to show any modified gravity effects on stellar structure at the background level and so one would expect the terms proportional to derivatives of ϕ_0 to be negligible and hence that the oscillation frequencies are identical to GR, however, this is not necessarily true at the level of perturbations and scalar radiation may provide an observational test. We will not investigate this possibility here but postpone it for future work.

IV. PROPERTIES OF THE MODIFIED LINEAR ADIABATIC WAVE EQUATION

The MLawe describes the behaviour of stellar oscillations under modified gravity. There are two major differences with respect to the GR equation. Firstly, there are two additional terms in the homogeneous part, proportional to the first and second derivatives of the background field. When $r < r_{\text{s}}$ these are negligible and the homogeneous part behaves as it would in GR, however, these are comparable to the other terms when $r > r_{\text{s}}$ and encode the effect of modified gravity on wave propagation in the region exterior to the screening radius. Physically, the term proportional to $d\phi_0/dr$ acts as a varying enhancement of Newton's constant $G(r)$ given by equation (10) and the term proportional to $d^2\phi_0/dr^2$ can schematically be viewed as $dG(r)/dr$ and so it encodes the effect of a varying Newtonian force in the outer regions.

The second effect is a driving term proportional to $\beta_0 d\phi/dr$. This is clearly the effect of the fifth-force due to perturbations in the field. This was modeled by [53] as an inhomogeneous forcing term at a single frequency. Here it appears as coupling between the field and stellar perturbations: the stellar perturbations source the scalar field perturbations and vice versa. Physically, $\tilde{\phi}(r, t)$ corresponds to scalar radiation (or rather the flux $T_{\phi 0i}$ at infinity). There is evidence from previous studies [53, 54] that this is negligible in chameleon-like systems and so from here on we will neglect the dynamics of the field perturbations and treat only the homogeneous part of the MLawe (48). There may, nevertheless, be interesting features associated with the coupled oscillator-like problem such as beating and scalar radiation and this is left for future work.

A. Boundary Conditions

The MLawe requires two boundary conditions in order to fully specify the solution given a specific value of ω [55]. Firstly, our system is spherically symmetric and so we must impose $\delta r = 0$ at $r = 0$. The MLawe then requires

$$\left. \frac{d\xi}{dr} \right|_{r=0} = 0. \quad (53)$$

The surface boundary condition depends on the stellar atmosphere model (see [56] for a discussion) but the lowest modes, where the period of oscillation is far longer than the inertial response time of the atmosphere can be described by solutions with $P(R) = 0$ so that $\delta P(R) = 0$. This gives the surface condition [56]

$$\left. \frac{\delta P}{P_0} \right|_{r=0} = \left(\frac{\omega^2 R^3}{GM} + 4 \right) \zeta(R), \quad (54)$$

where the Lagrangian pressure perturbation is given by (34). Note that the additional terms in the MLawe vanish at the stellar centre and radius if we take $\rho_0(R) = 0$ so that these conditions are identical to GR.

B. Sturm-Liouville Nature of the Equation

The MLawe can be written in Sturm-Liouville form

$$\hat{\mathcal{L}}\xi + w(r)\omega^2\xi = 0 \quad (55)$$

where the weight function $w(r) = r^4\rho_0(r)$ and the operator can be written

$$\hat{\mathcal{L}}^{\text{GR}} = \frac{d}{dr} \left(r^4 \Gamma_{1,0} P_0 \frac{d}{dr} \right) + r^3 \frac{d}{dr} [(3\Gamma_{1,0} - 4) P_0], \quad (56)$$

$$\hat{\mathcal{L}}^{\text{MG}} = \hat{\mathcal{L}}^{\text{GR}} - \frac{\beta\rho_0}{M_{\text{pl}}} r \frac{d^2\phi_0}{dr^2} - 2 \frac{\beta\rho_0}{M_{\text{pl}}} \frac{d\phi_0}{dr}. \quad (57)$$

The problem of finding the pulsation frequencies is then one of finding the eigenvalues of these equations that correspond to eigenfunctions satisfying the boundary conditions (53) and (54). In practice, it is not possible to solve these equations analytically for physically realistic stars and numerical methods must be used. We will do just this in section VI. Despite the need for numerics, a lot of the new modified gravity features can be discerned and elucidated using well-known Sturm-Liouville techniques and so we shall investigate these first.

C. Scaling Behaviour of the Eigenfrequencies

Using the dimensionless quantities:

$$\bar{P}_0(r) \equiv \frac{R^4}{GM^2} P_0(r), \quad (58)$$

$$\bar{\rho}_0(r) \equiv \frac{R^3}{M} \rho_0(r) \quad \text{and} \quad (59)$$

$$x \equiv \frac{r}{R}, \quad (60)$$

the MLawe (48) can be cast into dimensionless form:

$$\frac{d}{dx} \left(x^4 \Gamma_{1,0} \bar{P}_0 \frac{d\xi}{dx} \right) \quad (61)$$

$$+ x^3 \frac{d}{dx} [(3\Gamma_{1,0} - 4) \bar{P}_0] \xi + x^4 \bar{\rho}_0 [\Omega^2 - 4\pi\alpha \bar{\rho}_0] = 0, \quad (62)$$

where

$$\Omega^2 \equiv \frac{\omega^2 R^3}{GM} \quad (63)$$

is the dimensionless eigenfrequency and the term proportional to α is only present when $r > r_s$. In GR, $\alpha = 0$ and one can solve this given some equilibrium stellar model to find Ω^2 . Since this must be a dimensionless number one has $\omega^2 \propto GM/R^3$. In MG, there are two sources of change to this value at fixed mass: the change due to the different equilibrium structure described by (24) and the change due to the additional term in the MLawe. At the level of the background, we expect that stars of fixed mass have smaller radii and larger values of $\langle G \rangle$ (where by $\langle \rangle$ we mean some appropriate average over the entire star) so that the frequencies are higher in MG and at the level of perturbations, one can replace Ω^2 in the GR equation by the effective frequency $\Omega^2 - 4\pi\alpha \langle \bar{\rho}_0 \rangle$ so that $\Omega_{\text{MG}}^2 \approx \Omega_{\text{GR}}^2 + 4\pi\alpha \langle \bar{\rho}_0 \rangle$ and we therefore expect the MG eigenfrequency to be larger still.

The behaviour and importance of each effect requires a full numerical treatment, however, one can gain some insight by considering scaling relations when the star is fully unscreened so that $G \rightarrow G(1 + \alpha)$. The equations of stellar structure are self-similar so that we can replace each quantity, such as the pressure, by some characteristic quantity, in this example the central pressure P_c ,

multiplied by some dimensionless function in order to see how these different characteristic quantities scale when others are varied. Let us assume an equation of state of the form

$$P = K \rho^\gamma, \quad (64)$$

where K is a constant and γ differs from $\Gamma_{1,0}$ since the system need not be adiabatic. In this case, equations (23) and (24) give

$$\rho_c \propto \frac{M}{R^3} \quad (65)$$

$$\rho_c^{\gamma-1} \propto \frac{GM^2}{R}, \quad (66)$$

which can be combined to find the scaling of the radius for a fully-unscreened star in MG:

$$\frac{R_{\text{MG}}}{R_{\text{GR}}} = (1 + \alpha)^{-\frac{1}{3\gamma-4}} \quad (67)$$

at fixed mass. Ignoring the MG perturbations, one would then expect

$$\frac{\omega_{\text{MG}}^2}{\omega_{\text{GR}}^2} = (1 + \alpha)^{\frac{3\gamma-1}{3\gamma-4}}. \quad (68)$$

We shall confirm this limit numerically for some simple models later in section VI A. In the fully unscreened limit, we would then expect the eigenfrequencies to scale approximately like

$$\frac{\omega_{\text{MG}}^2}{\omega_{\text{GR}}^2} \sim (1 + \alpha)^{\frac{3\gamma-1}{3\gamma-4}} \left(1 + \frac{4\pi\alpha}{\Omega_{\text{GR}}^2} \langle \bar{\rho}_0 \rangle \right) \quad (69)$$

so that they are always larger than the GR prediction, at least when $\omega_{\text{GR}}^2 > 0$.

V. STELLAR STABILITY

Given the Sturm-Liouville nature of the problem, we can find an upper bound on the fundamental frequency ω_0 using the variational principle. Given an arbitrary trial function $\Psi(r)$, one can construct the functional

$$F[\omega] \equiv - \frac{\int_0^R dr \Psi^*(r) \hat{\mathcal{L}} \Psi(r)}{\int_0^R dr \Psi^*(r) \Psi(r) \rho_0 r^4}, \quad (70)$$

which has the property that $\omega_0^2 \leq F[\omega]$. Ignoring MG for now and taking the simplest case where χ is constant, the fundamental eigenfrequencies of the LAWE (49) satisfy

$$\omega_0^2 \leq \frac{\int_0^R dr 3r^2 (3\Gamma_{1,0} - 4) P_0}{\int_0^R dr \rho_0 r^4}. \quad (71)$$

When the right hand side is negative we have $\omega_0^2 < 0$ and the eigenfunctions have growing modes. This is the

well-known result in stellar astrophysics that stars where the adiabatic index falls below $4/3$ are unstable to linear perturbations and cannot exist[57].

In modified gravity, we have

$$\omega_0^2 \leq \frac{\int_0^R dr 3r^2 [(3\Gamma_{1,0} - 4)P_0] + \frac{\beta\rho_0}{M_{\text{pl}}} \left(r^4 \frac{d^2\phi_0}{dr^2} + 2r^3 \frac{d\phi_0}{dr} \right)}{\int_0^R dr \rho_0 r^4} \quad (72)$$

and so this stability condition is altered in stars which are at least partially unscreened. This is not surprising given the form of equation (48). The term proportional to the derivative of $[(3\Gamma_{1,0} - 4)P_0]$ behaves like a position dependent mass for ξ , which is negative when $\Gamma_{1,0} < 4/3$ so that one would expect growing modes. The additional terms in (72) are due to the two new terms in (48), which are of precisely the same varying mass form with the opposite sign. A negative mass, which would signify an instability, coming from the GR term can then be compensated by the new terms in MG, restoring stability[58].

Physically, the adiabatic index is a measure of how the pressure responds to a compression of the star. Given a compression from one radius R_1 to a smaller radius R_2 , a larger adiabatic index will result in more outward pressure. If this increase in pressure is faster than the increase in the gravitational force, the star can resist the compression and is hence stable. Below the critical value of $4/3$, the converse is true and the star is unstable. We have already seen above that the new terms contributing to the stability correspond to a varying value of G and its derivative in the outer layers. Since modified gravity enhances the gravity, one may naïvely expect that its effect is to destabilise stars, however, we will argue below that this is not the case. The MLawe describes acoustic waves propagating in the star. If the gravity and its gradient is larger in the outer layers then it is more difficult for these waves to propagate and hence modes which would usually have been unstable are stabilised.

Once again, we must disentangle the effects of the modified equilibrium structure and the perturbations on the critical value of $\Gamma_{1,0}$. Consider first the modified equilibrium structure only. In this case, the stability condition is given by the GR expression, equation (71), however the pressure and density profiles will be different. Clearly, the critical value for the instability is still $4/3$ since this is the only value which makes the integral vanish but this does not necessarily mean the stability is altered away from this value. Scaling the pressure and density using the dimensionless quantities defined in (58), (59) and (60), we have

$$\omega_0^2 \leq (3\Gamma_{1,0} - 4) \frac{GM}{R^3} f(\chi_0), \quad (73)$$

where f is a dimensionless function which depends on the composition of the star[59]. In MG, the radius of the star will be smaller than its GR counterpart and the effective value of G is larger. Hence, when $\Gamma_{1,0} > 4/3$ the maximum possible frequency is greater than in GR whereas

when $\Gamma_{1,0} < 4/3$ the maximum frequency is more negative. If a star is unstable in GR then MG enhances the instability, moving the frequency further away from zero. This can also be seen from the scaling relation (68). If $\omega_{\text{GR}}^2 < 0$ then ω_{MG}^2 is even more negative. At the background level, the effects of MG are to destabilise stars that are already unstable, without altering the stability condition.

Let us now turn our attention to the effects of perturbations. Using equation (50), we have

$$\omega_0^2 \leq \frac{\int_0^R dr 3r^2 [(3\Gamma_{1,0} - 4)P_0] + \int_{r_s}^R 4\pi\alpha Gr^4 \rho_0^2}{\int_0^R dr \rho_0 r^4}. \quad (74)$$

The additional term is clearly positive and so one may lower the value of $\Gamma_{1,0}$ below $4/3$ and still find positive eigenfrequencies, confirming our earlier intuition that the effect of MG is to stabilise stars compared with GR. Unlike GR, there is no universal critical index in MG and a numerical treatment is necessary to extract the value for a star of given composition and screening radius. We will investigate the stability of some simple semi-analytic models in section VIA 2 but before doing so, one can gain some insight into the full effects of MG on the stability by using the same scaling relations as section IV C. In particular, we can set the numerator in (74) to zero to find the modified critical index:

$$\Gamma_{1,0}^{\text{critical}} = \frac{4}{3} - g(\chi_0)\alpha, \quad (75)$$

where g is a dimensionless number which encodes the effects of the structure and composition of the star. In $f(R)$ theories, $\alpha = 1/3$ [39] and so we expect the critical value of $\Gamma_{1,0}$ to change by $\mathcal{O}(10^{-1})$ assuming that $g \sim \mathcal{O}(1)$. We will verify numerically that this is indeed the case for a simple model in section VIA 2.

VI. NUMERICAL RESULTS

We will now proceed to solve the MLawe for various different stars. We will do this for two different stellar models: Lane-Emden models, which describe the equilibrium configuration of spheres of gas collapsing under their own gravity, and MESA models, which are fully consistent and physical models that include effects such as nuclear burning networks, metallicity, convection, energy generation and time-evolution. The first models are simple compared to the second but they have the advantage that the non-gravitational physics (e.g. nuclear burning) is absent, which will allow us to gain a lot of physical intuition about the new modified gravity features. They are simple semi-analytic models and this allows us to first investigate the MLawe using a controlled system with known scaling properties and limits without the complications arising from things like radiative transfer. This also allows us to test that the code is working correctly since we can compare our results with both the

GR case, which has been calculated previously, and the fully unscreened case, which can be predicted analytically given the GR one. Their perturbations can also be described using an arbitrary value of $\Gamma_{1,0}$, independent of their composition and so we will use them to study the modifications to stellar stability. These models are not realistic enough to compare with observational data and the power of MESA lies in that it can produce realistic models of stars such as main-sequence and Cepheid stars, which will allow us to predict the effects of MG on realistic stars in unscreened galaxies. MESA predictions have already been used to obtain the strongest constraints on chameleon-like models [27] and combining these models with the modified gravity oscillation theory has the potential to provide new constraints.

The details of the implementation of MG into MESA is given in Appendix A (see also [26, 27] for some previous uses of the same code) and, where necessary, details of the numerical procedure used to solve the MLawe are given in Appendix B. The shooting method has been used to solve the MLawe in all instances.

A. Lane-Emden Models

Lane-Emden models describe spheres of gas that support themselves against gravitational collapse by producing an outward pressure given by the solution of the (in our case modified) hydrostatic equilibrium equation. The key assumption is that the radiation entropy per unit mass is constant, which decouples the effects of nuclear burning (26) and radiative transfer (25) from the stellar structure equations derived in section (III A). In this case, only the mass-conservation equation (23) and the hydrostatic equilibrium equation (24) are relevant. In GR, these equations are self-similar, which allows one to scale out the physical quantities in favour of dimensionless ones but this property is lost if one assumes a modified gravity profile of the form (10) and so, in order to retain a comparison with the GR case, we will solve the modified hydrostatic equilibrium equation

$$\frac{dP_0}{dr} = \frac{GM(r)\rho_0(r)}{r^2} \begin{cases} 1 & r < r_s \\ (1 + \alpha) & r > r_s \end{cases}, \quad (76)$$

which physically corresponds to setting $G \rightarrow G(1 + \alpha)$ in the region exterior to the screening radius. Lane-Emden models describe *polytropic gases* defined by

$$P_0(r) = K\rho_0^{\frac{n+1}{n}}, \quad (77)$$

where K is constant for a star of given mass but varies between different stars. n , is known as the *polytropic index*. The case $n = 3$ was studied in [26]; here we shall generalise their procedure to arbitrary values. We can eliminate r in terms of the Lane-Emden coordinate $y = r/r_c$ [60] where r_c is defined by

$$r_c^2 \equiv \frac{(n+1)P_c}{4\pi G\rho_c^2}, \quad (78)$$

where P_c and ρ_c are the central pressure and density respectively. Next, we re-write the pressure and density in terms of a dimensionless function $\theta(y)$ such that $P_0 = P_c\theta^{n+1}$ and $\rho_0 = \rho_c\theta^n$. Substituting this into the mass conservation and modified hydrostatic equilibrium equations (equations (23) and (24) respectively) we can combine to two to find the modified Lane-Emden Equation:

$$\frac{1}{y^2} \frac{d}{dy} \left[y^2 \frac{d\theta}{dy} \right] = - \begin{cases} (1 + \alpha)\theta^n, & y > y_s \\ \theta^n, & y < y_s \end{cases}, \quad (79)$$

where y_s is the Lane-Emden screening radius such that $r_s = r_c y_s$. The boundary conditions for this equation are $\theta(0) = 1$ ($P_0(0) = P_c$) and $d\theta/dy(0) = 0$ (this follows from the fact that $M(0) = 0$ in the hydrostatic equilibrium equation). The radius of the star in Lane-Emden coordinates, y_R is then found from the condition $\theta(y_R) = 0$ (the pressure is zero at the stellar radius), from which the physical radius, $R = r_c y_R$ may be found. For convenience, we introduce the quantities

$$\omega_R \equiv -y_R^2 \frac{d\theta}{dy} \Big|_{y=y_R} \quad \text{and} \quad (80)$$

$$\omega_s \equiv -y_s^2 \frac{d\theta}{dy} \Big|_{y=y_s}. \quad (81)$$

In GR, $\alpha = \chi_0 = 0$ and there is a unique solution for any given value of n . We will denote the GR values of y_R and ω_R using \bar{y}_R and $\bar{\omega}_R$ respectively. In MG, there is a two-dimensional space of solutions at fixed n given by specific values of χ_0 and α , each with different values of ω_R , ω_s , y_s and y_R .

By writing equation (12) in Lane-Emden variables, we find an implicit relation for ω_s and hence the screening radius:

$$\frac{\chi_0}{GM/R} \equiv X = \left[\frac{y_R\theta(y_s) + \omega_R - \frac{y_R}{y_s}\omega_s}{\omega_R + \alpha\omega_s} \right], \quad (82)$$

where

$$M = \int_0^R 4\pi r^2 \rho_0(r) dr = 4\pi r_c^3 \rho_c \left[\frac{\omega_R + \alpha\omega_s}{1 + \alpha} \right]. \quad (83)$$

As $r_s \rightarrow 0$, the star becomes increasingly unscreened, $\omega_s \rightarrow 0$ and $\theta(y_s) \rightarrow 1$. This gives the maximum value of X where the star is partially screened. For values greater than this, equation (82) has no solutions and the star is always unscreened. From (82), we have

$$X_{\max} = \frac{y_R + \omega_R}{\omega_R} \quad (84)$$

independent of α . Later on, we will specify to the case $n = 1.5$ so for future reference we note here that $X_{\max} \approx 2.346$.

1. Perturbations of Lane-Emden Models

We solve the MLAWE by first tabulating solutions of the modified Lane-Emden equation and using this to numerically solve the MLAWE. This is achieved using the shooting method and the full numerical details are given in appendix B. The dimensionless eigenvalues

$$\tilde{\omega}^2 \equiv \frac{(n+1)\omega^2}{4\pi G\rho_c} \quad (85)$$

for Lane-Emden models in GR were numerically calculated in 1966 by [61] and so as a code comparison, we have compared our fundamental frequencies and first overtones with theirs for different values of n and $\Gamma_{1,0}$. Their values are given to five decimal places and in each case our results matched with theirs to this accuracy.

Despite our approximation of a constant enhancement of G in the region exterior to r_s , self-similarity is not preserved completely in MG and so one cannot compare solutions for fixed $\chi_0/(GM/R)$. Given a star in GR of mass M and radius R , one must decide upon the correct comparison in MG. In what follows, we will fix the mass and composition (this implies that K is fixed) of the star and allow the radius to vary so that the stars we compare are stars of the same mass whose radii (and pressure and density profiles) have adjusted to provide an equilibrium configuration given a specific value of χ_0 (and hence r_s) [62]. In order to fix the mass, one must fix the central density and so in MG we have $\rho_c = \rho_c(\chi_0, \alpha)$, highlighting the consequences of breaking self-similarity. For concreteness, we will work with $n = 1.5$. This is a good approximation to stellar regions which are fully convective (see [63], sections 7 and 13 for more details) and hence have physical applications to red giant and Cepheid stars. In terms of an equation of state of the form (64), this model corresponds to $\gamma = 5/3$. In what follows, we will assume that γ is identical to the adiabatic index and set $\Gamma_{1,0} = 5/3$, however, we will relax this assumption when considering stellar stability and allow for more general models.

Using equation (83), we have

$$\rho_c = \left(\frac{M}{4\pi}\right)^2 \left[\frac{8\pi G}{2K}\right]^3 \left(\frac{1+\alpha}{\omega_R + \alpha\omega_s}\right)^2, \quad (86)$$

which may be used to find the modified Mass-Radius- χ_0 relation (as opposed to the Mass-Radius relation found in GR).

$$R = \frac{1}{(4\pi)^{\frac{3}{2}}} \left(\frac{5K}{2G}\right) \left(\frac{\omega_R + \alpha\omega_s}{1+\alpha}\right)^{\frac{1}{3}}. \quad (87)$$

In the cases of red giant stars and low-mass Cepheids, we have $GM/R \sim 10^{-7}$ and so we can pick $M = M_{\text{GR}}$ and $R = R_{\text{GR}}$ in the GR case ($\alpha = 0$) such that $GM_{\text{GR}}/R_{\text{GR}} = 10^{-7}$ and

$$\frac{GM}{R} = 10^{-7} \left(\frac{M_{\text{GR}}}{M}\right) \left(\frac{R}{R_{\text{GR}}}\right) \quad (88)$$

and equation (82) is (fixing $M = M_{\text{GR}}$)

$$\frac{\chi_0}{10^{-7}} = \frac{\bar{y}_R}{y_R} \left[\frac{y_R \theta(y_s) + \omega_R - \frac{y_R}{y_s} \omega_s}{(\bar{\omega}_R(1+\alpha))^{\frac{1}{3}} (\omega_R + \alpha\omega_s)^{\frac{2}{3}}} \right]. \quad (89)$$

The procedure is then as follows: Given a specific value of χ_0 , we use a trial value of y_s to solve the Modified-Lane Emden equation until equation (89) is satisfied. We then use the Lane-Emden solution in the MLAWE to numerically calculate the value of $\tilde{\omega}^2$ given a value of $\Gamma_{1,0}$. Using equation (86), we can find the ratio of the period in MG to that predicted by GR:

$$\frac{\tau_{\text{MG}}}{\tau_{\text{GR}}} = \sqrt{\frac{\tilde{\omega}_{\text{GR}}^2}{\tilde{\omega}_{\text{MG}}^2} \frac{\omega_R + \alpha\omega_s}{\bar{\omega}_R(1+\alpha)}}. \quad (90)$$

We can then calculate this ratio for any values of χ_0 and α .

Before presenting the numerical results, it is worth noting that the fully-unscreened behaviour of the star, at least in the case where only the effects of the modified equilibrium structure are considered, can be calculated in terms of the GR properties of the star. In the fully-unscreened case, one has $\omega_s = y_s = 0$. One can then set $y \rightarrow (1+\alpha)^{-\frac{1}{2}}y$ to bring equation (79) into the same form as in GR. This then gives $y_R^{\text{unscreened}} = (1+\alpha)^{-\frac{1}{2}}\bar{y}$ and $\omega_R^{\text{unscreened}} = (1+\alpha)^{-\frac{1}{2}}\bar{\omega}_R$. For $n = 1.5$, one has $\bar{y}_R \approx 3.654$ and $\bar{\omega}_R = 2.72$. One then has, by rescaling the MLAWE (see Appendix B for the equation in these coordinates), $\tilde{\omega}_{\text{unscreened}}^2/\tilde{\omega}_{\text{GR}}^2 = (1+\alpha)$ and so, using (86), $\omega_{\text{unscreened}}^2/\omega_{\text{GR}}^2 = (1+\alpha)^4$, which exactly matches our prediction in (68) for $\gamma = 5/3$. From equation (90), we have $\tau_{\text{MG}}^{\text{unscreened}}/\tau_{\text{GR}} = (1+\alpha)^{-2} = 0.5625$ for $\alpha = 1/3$. These unscreened results can be used to check that the numerical results are behaving as expected.

We would like to investigate the effect of the different modifications coming from the altered equilibrium structure and the modified perturbation equation separately. They appear at the same order in the MLAWE and so we expect them to contribute equally and it is important to dis-entangle their effects, especially since we have already argued in section V that they may contribute differently to the stellar stability and that the equilibrium structure acts to make negative GR frequencies more negative. Lane-Emden models are perfectly suited for this study since we do not have to worry about altered evolution histories and so we will consider two cases:

- case 1: We solve the LAWE (49) using modified Lane-Emden profiles. This case only includes the modified equilibrium structure.
- case 2: We solve the full MLAWE using both the modified background structure and the modified perturbation equations. This is the physically realistic case.

The case where we ignore the modified equilibrium structure and include only the perturbations is highly unphysical, there is no screening radius and so we are introducing the perturbations about an arbitrary radius. Furthermore, the size of the effect depends on whether we take the radius of the star as corresponding to the GR solution (in which case we are ignoring the effects on the period coming from the change in the critical density (86)) or the equivalent MG solution (in which case our profiles do not satisfy the boundary conditions and we are including some of the modified equilibrium properties in our analysis). For these reasons, we do not investigate this scenario. In each case, we assume the profile (10). Since we have solved the modified Lane-Emden equation with constant α in the region $r > r_s$ (this is required for a physically meaningful comparison with GR) this profile is not technically correct since it does not satisfy the stellar structure equations. In fact, it is an under-estimate [64]. In each case we will fix $\alpha = 1/3$, corresponding to $f(R)$ gravity and vary χ_0 .

In figure 1 we plot the ratio of the MG period to the GR one as a function of $\log \chi_0$ for case 1. In a previous study [27], the approximation

$$\frac{\tau_{\text{MG}}}{\tau_{\text{GR}}} = \sqrt{\frac{G}{\langle G \rangle}}, \quad (91)$$

where $\langle G \rangle$ is the average value of the effective Newtonian constant using some appropriate weighting function was used in order to obtain new constraints on the model parameters. This approximation is based on the change in the equilibrium structure only and so it is important to test not only how it compares with the predictions from the full numerical prediction at the background level but also how well it can be used to approximate the frequency once MG perturbations are taken into account. Hence, we also plot the approximation using the Epstein [65] weighting function as was used by [27]. In each case we have calculated $\langle G \rangle$ using the modified Lane-Emden solution at given χ_0 . One should emphasise that [27] used this approximation for MESA models whereas this comparison is purely for the hypothetical case of Lane-Emden models. We will investigate how well this holds for MESA models in section VIB. The figure reveals that the approximation (91) is an over-estimate for very screened stars whereas it is a large under-estimate for stars that are significantly unscreened. The Epstein function favours the regions of Cepheid stars that are most important for pulsations. This tends to be the outer layers and so it is no surprise that it over-estimates the effects in the screened case: it places a large emphasis on the small region where the gravity is enhanced even though this region has little to no effect on the structure of the star. The approximation (91) assumes that the stellar radius is fixed but in Lane-Emden models this is clearly a decreasing function of χ_0 and α according to (87). According to (63), the period scales as $R^{\frac{3}{2}}$, which explains why the approximation is an underestimate when the star is very unscreened and the change in

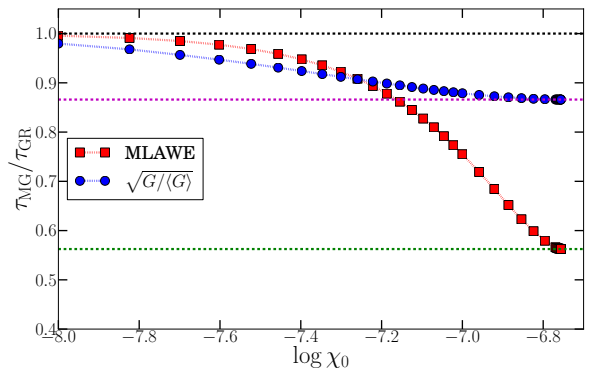


FIG. 1. The fractional change in the stellar pulsation period as a function of $\log_{10} \chi_0$ when only the change to the equilibrium structure is considered (case 1). The red squares correspond to eigenfrequencies of the LAWE whereas the blue circles show the approximation (91). The green dashed line shows the ratio for a fully unscreened star and the black dashed line shows a ratio of 1, corresponding to a GR star. The magenta line shows the fully-unscreened value of $\sqrt{\frac{G}{\langle G \rangle}} = (1 + \alpha)^{-\frac{1}{2}}$.

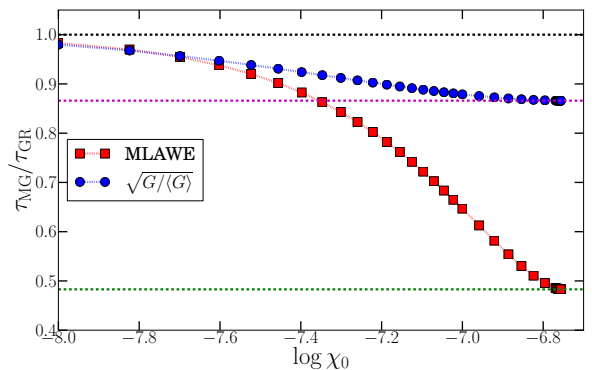


FIG. 2. The fractional change in the stellar pulsation period as a function of $\log_{10} \chi_0$ when both the effects of the modified equilibrium structure and modified perturbation equation are considered (case 2). The red squares correspond to eigenfrequencies of the MLAWE whereas the blue circles show the approximation (91). The green dashed line shows the ratio for a fully unscreened star and the black dashed line shows a ratio of 1, corresponding to a GR star. The magenta line shows the fully-unscreened value of $\sqrt{\frac{G}{\langle G \rangle}} = (1 + \alpha)^{-\frac{1}{2}}$.

the radius is significant. We can also see that the ratio asymptotes to the value predicted above when the star is fully-unscreened.

In figure 2 we plot the ratio of the MG period to the GR one for case 2. We can see that the approximation (91) fails very rapidly and that the change in the period is significant and can be as large as 50% for significantly unscreened stars.

We then plot the two cases together in figure 3. One

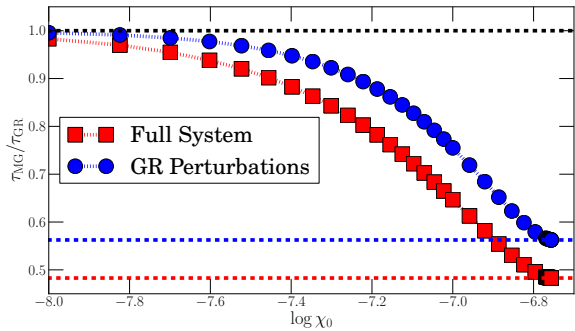


FIG. 3. The fractional change in the stellar pulsation period as a function of $\log_{10} \chi_0$ for case 1 (blue circles) and case 2 (red squares). The black dashed line shows the GR ratio of 1 and the red and blue lines show the fully-unscreened ratio for the full simulation and the one including only the modified equilibrium structure respectively.

can see that the effect of the new terms coming from the modified structure of hydrodynamics has a significant effect on the period and that if one were to consider only the background structure, the change in the period would be a large under-estimate. That being said, the change in the period from the GR value is $\mathcal{O}(1)$ as soon as one calculates using the modified equilibrium structure and the effect of the perturbation is to increase this by an amount not as large as this initial change. These results seem to suggest that convective stars such as Cepheid and red giants may show very large changes in the oscillation periods due to their modified background structure and that the approximation will tend to under-estimate this change. Furthermore, the effects of the hydrodynamic perturbations will make these changes more drastic but not as large as those coming from the modified background. In fact, we will see below that this is not the case for Cepheid models. We will see that the approximation holds very well when only the background structure is considered but when the perturbations are included the resulting change in the period is three times as large as that due to the modified equilibrium structure alone. One assumption we have made here is that the constant K appearing in the polytropic relation is constant. This is tantamount to having a uniform composition throughout the entire star. This is a good approximation for red giant stars, which are fairly homogeneous but Cepheids have shells of varying composition and several ionised layers and so this is likely not an accurate approximation. In particular, we will see below that the radius of Cepheid stars does not change significantly in MG, contrary to what this model would predict and this is why we find the approximation holds well despite this models predictions.

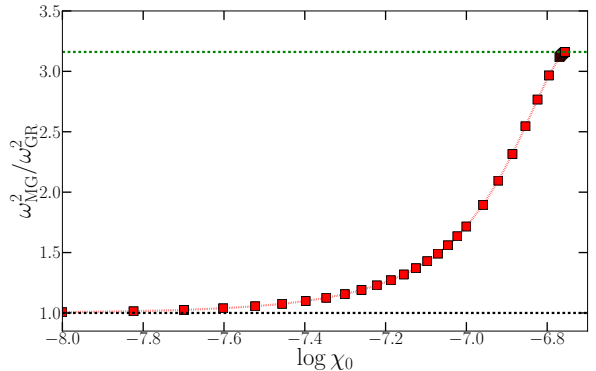


FIG. 4. The ratio of the MG to GR eigenfrequencies as a function of $\log_{10} \chi_0$ when $\Gamma_{1,0} \approx 1.2333$.

2. Stability of Lane-Emden Models

Before moving on to look at realistic models from MESA, we will first use Lane-Emden models to investigate the modification to the stellar stability criterion. In section V we derived the new properties relating to stellar stability in MG and argued two new features: first, that when there are unstable modes present in GR such that $\omega_0^2 < 0$, then, when only the change equilibrium structure is taken into account, the instability is worse i.e. ω_0^2 is more negative; second, that the new term appearing in the MLawe makes stars more stable, the critical value of $\Gamma_{1,0}$ required for $\omega_0^2 < 0$ is less than the GR value of $4/3$ and the correction is of order $g(\chi_0)\alpha$ given in (75). $g(\chi_0)$ encodes the competing effects of the new term in the MLawe and the modified structure and composition coming from the new equilibrium structure. Here, we will verify these predictions numerically.

In order to investigate the first, we have solved for the modified eigenfrequencies of the same $n = 1.5$ modified Lane-Emden model investigated in the last subsection ignoring the new term in the MLawe and using various values of $\Gamma_{1,0} < 4/3$. This corresponds to a star whose adiabatic perturbations are governed by a different index to that appearing in the equation of state that fixes the equilibrium structure. In each case, the modified eigenfrequencies are indeed more negative the more unscreened the stars are and, as an example, we plot the ratio $\omega_{MG}^2/\omega_{GR}^2$ in the case $\Gamma_{1,0} = 37/30 \approx 1.23333$, which is close to being stable. In this case one has $\omega_{GR}^2 = -0.314$ and so the larger this ratio, the more negative the MG value. This is plotted in figure 4 and it is evident that the instability is indeed worse in stars which are more unscreened.

Next, we turn our attention to the modification of the critical value of $\Gamma_{1,0}$. In order to investigate this, we again use the $n = 1.5$ model above and vary $\Gamma_{1,0}$ as a function of χ_0 . We scan through different values of $\Gamma_{1,0}$ at fixed χ_0 in order to find the value where $\omega^2 \approx 0$ (to 8 decimal places), which is the new critical value in MG. We solve for the

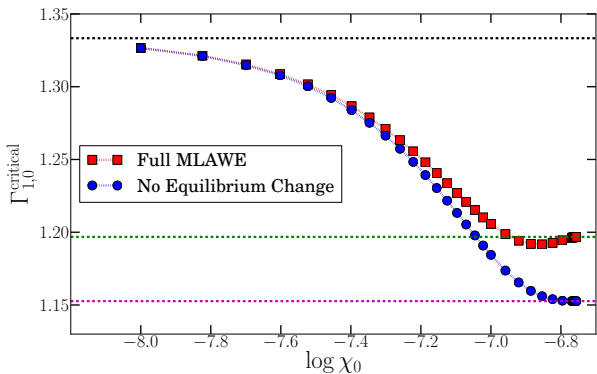


FIG. 5. The critical value of $\Gamma_{1,0}$ as a function of $\log_{10} \chi_0$. The blue circles show the critical values when the modifications to the equilibrium structure are ignored and the red squares show the critical values when the full MLawe is solved. The black dashed line shows the GR value of $4/3$ and the magenta and green lines show the fully unscreened values in the no modified equilibrium and full cases respectively.

zero-eigenfrequencies in two cases: the case where we ignore the modified equilibrium structure [66] and include only the MG perturbations and the full MLawe. The values of the critical value of $\Gamma_{1,0}$ vs $\log \chi_0$ are plotted in figure 5.

It is evident from the figure that the critical value is indeed lower than $4/3$ showing that these models are indeed more stable in MG. One can also see that the red curve lies above the blue one so that the effect of the modified equilibrium structure is to destabilise the star compared with how stable it would have been had only the modified perturbation structure been present. We have already argued this in equation (73), where we found that the contribution to the stability condition from the equilibrium structure is larger in MG gravity. In terms of the dimensionless function $g(\chi_0)$, (73) appears as a denominator and so the effect of the background is to reduce the correction to the GR critical index. The critical value when the modified background structure is ignored decreases monotonically, however, the full MLawe predicts an increase in stars that are significantly unscreened, showing that the effects of this altered equilibrium structure become more important when the star is more unscreened. This is consistent with our findings in the previous subsection. Finally, we note that the change in the critical index is indeed of order 10^{-1} , which we predicted using analytic arguments in section V.

B. MESA Models

Having studied some simple stellar models and gained some intuition about the MLawe, we now turn our attention to realistic stellar models from MESA, which provides consistent stellar models including the full effects of modified gravity. The implementation of modified grav-

ity into MESA is discussed in appendix A. We will limit the discussion to Cepheid stars, which are useful observational tools to study modified gravity and have already been used to place the strongest constraints on χ_0 and α to date [27]. They are the only stars whose oscillations can be observed in distant galaxies [67].

1. Perturbations of Cepheid Models

[27] have used the perturbed period-luminosity relation (15) with the approximation $\Delta\tau/\tau \approx \Delta G/2G$, where $\Delta G \equiv \langle G \rangle - G$ is found using the Epstein [65] function, to find the difference between the inferred distances in MG and GR. We are now in a position to calculate $\Delta\tau/\tau$ for the same models which they have used and check how well this approximation holds. In table 1 they present six models with different χ_0 and α for a $6M_\odot$ star with initial metallicity $z = 0.004$. Using MESA, we have recreated these models using the same procedure that they outline. Using the instability strip given by [68],

$$\log L = 4.2 - 46(\log T_e - 3.8) \quad (92)$$

for the blue edge we select first-crossing models [69] using their different parameter values and an additional model where the star has evolved under GR. The red-edge is determined by a dissipation term in the LAWE due to convection, which we have not included, and so we do not make any statements about red-edge properties. We then check that our models agree with theirs by calculating $\Delta G/G$ and we indeed find the same values. Next, we calculate the modified periods by solving the MLawe and we again examine both the full solution and the solution where we ignore the MG perturbations in order to discern their new effects. The models with $\alpha = 1/3$, $\chi_0 = 10^{-6}$, $\alpha = 1/2$, $\chi_0 = 10^{-6}$ and $\alpha = 1$, $\chi_0 = 4 \times 10^{-7}$ all execute one loop that does not cross the instability strip and cross only on the second loop. There is hence no model to compare to the GR first-crossing and so we do not analyse these models [70].

In table I we show $\Delta\tau/\tau$ calculated for each of their models using the approximation, the case of MG perturbations turned off and the full MLawe. In each case, the change in the radius is $\Delta R/R \sim \mathcal{O}(10^{-2})$ and so most of the change in the period is due to modified gravity and not the size of the star. This is very different from the $n = 1.5$ Lane-Emden model in subsection VI A 1 which predicts a large reduction in the radius when the star is unscreened. It is hardly surprising then that the approximation works very well when the MG perturbations are ignored; this approximation was found by perturbing the relation $\tau \propto G^{-\frac{1}{2}}$ at fixed radius. When the MG perturbations are included, we see that this approximation breaks down and the relative difference in the period is $\mathcal{O}(10^{-1})$, which is approximately a day. Table II shows how these changes propagate to $\Delta d/d$, which is the astrophysical quantity used to place constraints. Again, we see that the approximation is good when one ignores

the MG perturbations but when these are included the relative distance difference can be up to three times as large. We therefore conclude that the constraints of [27] are conservative, and it is possible that they could be improved given the larger change predicted in the full theory.

With this in mind, we estimate the values of χ_0 that can be probed using the full MLawe rather than the approximation for the same values of α discussed above. We accomplish this by taking the same initial stellar conditions and running a series of new simulations using MESA for successively decreasing values of χ_0 . Using the same procedure to identify the Cepheid models at the blue edge as described above, we calculate $\Delta d/d$ using the MLawe until it is equal to the value predicted by the approximation. These values were those used in [27] to obtain their constraints. In table III we show the values of χ_0 and α such that the MLawe gives the same result as the approximation. These represent an estimate on the range of parameters that one could hope to constrain using the same data-sets and the MLawe. Of course, this is just a simple estimate and a more rigorous method would be to redo their analysis, which is beyond the scope of this work. Nevertheless, this simple estimate goes to show that we can expect new constraints significantly stronger than the previous ones, in particular, the MLawe predictions suggest that the constraints could be pushed into the $\mathcal{O}(10^{-8})$ regime.

VII. DISCUSSION AND CONCLUSION

We have presented a study of the properties of stellar oscillations in modified theories of gravity such as chameleons and symmetrons. Starting with a generic fifth-force appropriate for all couplings of a scalar to matter of the form $\mathcal{L}_{\text{coupling}} = C(\phi)T_m$, we have derived the equations of modified gravity hydrodynamics. At zeroth-order, these give us the modified equations of stellar structure, which have been well-studied before [25–27]. At first-order, we obtain the equations of motion describing radial and adiabatic perturbations of the star coupled to perturbations of the scalar field. This describes scalar radiation which is known to be small and so we ignore the coupling terms to find the equations governing the oscillations of stars in modified gravity, the modified linear adiabatic wave equation. This is a Sturm-Liouville problem where the eigenvalues correspond to the angular frequency of oscillations. We have discerned two new features due to the modification of this equation: first, the period of oscillations is greatly reduced compared to what one would naïvely expect from considering the modified equilibrium structure alone and second, the adiabatic index, $\Gamma_{1,0}$, can be lowered below the GR limit of $4/3$ while keeping ω_0^2 , the fundamental frequency, positive so that there are no unstable modes. This means that stars are more stable in MG than in GR and, unlike GR, there is no universal bound on $\Gamma_{1,0}$ so that the value where

$\omega_0^2 = 0$ depends on the composition of the star as well as the MG parameters. We found that the modified equilibrium structure by itself could not alter the stability bound but it does have an effect on the new critical value of $\Gamma_{1,0}$ once the perturbations are included. Specifically, it raises it closer to the GR value relative to what it would have been if we had perturbed around the GR solution. Whilst the modified background structure cannot change the instability criterion alone, if an instability is present then it acts to make ω^2 more negative than the GR prediction.

After discussing these features in length, we have investigated them numerically. Using a generalisation of the procedure in [26], we have solved the MLawe for $n=1.5$ Lane-Emden models, which describe convective stars. We numerically calculated the change in the period as a function of χ_0 for $f(R)$ gravity ($\alpha = 1/3$) and found that it monotonically decreased. We found that the change in the equilibrium structure produced very large changes from the GR values and that these increase by a significant but smaller amount once the effects of modified gravity hydrodynamics are included. We discussed the application of this model to real stars and concluded that whilst likely appropriate for red giants, it is probably not a good approximation to Cepheid stars, especially in light of the results from MESA discussed below. Nevertheless, this is a useful model whose simplicity allowed us to gain a lot of intuition about the behaviour of the MLawe and how it responds to various MG features. In particular, it revealed how the effects of the modified hydrodynamic perturbations can be important if one wishes to calculate the correct oscillation period. Next, we investigated the stability properties of the models. We confirmed numerically that ω^2 is indeed more negative than predicted in GR when considering only the modified equilibrium structure. We then reintroduced the MG terms into the MLawe and used the same Lane-Emden models to numerically find the new critical value of $\Gamma_{1,0}$ as a function of χ_0 . We indeed found that this was always less than $4/3$ so that these stars are indeed more stable. When the equilibrium structure is ignored so that we perturb around the GR solution, this decrease is monotonic. When we then consider the full MLawe, the modified equilibrium structure acts to raise the critical value above what it would be if we had perturbed around GR but never to $4/3$. When the star is unscreened, the effects of the modified equilibrium structure begins to dominate and the critical value for very unscreened stars is not as small as some which are partially-screened.

Having gained a lot of intuition from these simple models, we turned our attention to models coming from MESA. MESA is a stellar structure code which can consistently simulate the structure and evolution of stars over their entire life and includes every important stellar process such as convection, mass-loss, nuclear burning, opacity tables etc. In [26], we presented a modified version which includes the effect of chameleon-like theories in a model

| α | χ_0 | $\Delta\tau/\tau$ (approximation) | $\Delta\tau/\tau$ (no perturbations) | $\Delta\tau/\tau$ (full MLAW) |
|----------|--------------------|-----------------------------------|--------------------------------------|-------------------------------|
| 1/3 | 4×10^{-7} | 0.086 | 0.092 | 0.266 |
| 1/2 | 4×10^{-7} | 0.054 | 0.064 | 0.207 |
| 1 | 2×10^{-7} | 0.102 | 0.122 | 0.314 |

TABLE I. The change in the period of Cepheid pulsations due to MG effects.

| α | χ_0 | $\Delta d/d$ (approximation) | $\Delta d/d$ (no perturbations) | $\Delta d/d$ (full MLAW) |
|----------|--------------------|------------------------------|---------------------------------|--------------------------|
| 1/3 | 4×10^{-7} | -0.03 | -0.04 | -0.12 |
| 1/2 | 4×10^{-7} | -0.05 | -0.06 | -0.16 |
| 1 | 2×10^{-7} | -0.06 | -0.07 | -0.19 |

TABLE II. The change in the inferred Cepheid distance due to MG. In each case $\Delta d/d$ was found using the perturbed P-L relation 15.

| α | χ_0 |
|----------|--------------------|
| 1/3 | 9×10^{-8} |
| 1/2 | 7×10^{-8} |
| 1 | 3×10^{-8} |

TABLE III. The lower bounds on χ_0 and α that could potentially be placed if one were to use the same procedure and data-sets as [27] using the full MLAW instead of the approximation.

independent way (see also [25] for a different implementation). This can be used to make quantitative predictions which can be compared to data. Indeed, this has already been done by [27] who used it to find approximations to the change in the period of Cepheid pulsations, which was then used to constrain χ_0 and α by comparing the distances to the same unscreened dwarf galaxies measured using Cepheid and tip of the red giant branch techniques.

Here, we have explored how the MG perturbations affect the periods of Cepheid pulsations. These stars are good probes of MG and here we have found that the perturbations do indeed alter the modified periods significantly. If we ignore the MG perturbations then our numerical calculation of $\Delta d/d$, the change in the inferred Cepheid distance, agrees very well with the approximation used in [27]. Once the perturbations were included, we found that this change could be up to three times as large as the approximation predicts.

Previous studies [27] have used this approximation and it is the astrophysical errors that limit the strength of the constraint. What we have shown here is that these constraints are conservative and it may be possible to reduce the bounds further using the same data-sets if one were to use the results from the full MLAW. In particular, we have estimated that one could probe the self-screening parameter to values of $\mathcal{O}(10^{-8})$ when $\alpha \sim \mathcal{O}(1)$, although this is by no means a rigorous statistical analysis and a more detailed treatment is left for future work.

The altered stability condition, whilst interesting, is unlikely to be a good probe of modified gravity in the near-future. The increased stability has very few observational consequences. For example, one might look for

physical processes where $\Gamma_{1,0}$ falls below 4/3. This is the case with type II supernovae, where the progenitor stars are very massive with large radiation pressures. Upon compression, the extra photon energy is used to photo-disintegrate iron nuclei and very little is transferred to the pressure so that $\Gamma_{1,0} < 4/3$. One might imagine then that the type II supernova rate in dwarf galaxies would be less if they were unscreened so that galactic processes like supernova feedback etc. are less efficient. Unfortunately, the current lack of complete models for type II supernovae and the fact that the feedback efficiency (and supernova rate) tend to be packaged into efficiency parameters (see, for example, [71, 72] and references therein) that are not necessarily physical makes a quantitative prediction that can be compared to observations difficult. That being said, one could potentially look for stars in dwarf galaxies which are not seen in the HR diagrams of stellar populations in our own galaxy. Such stars would likely be very massive and hence have high luminosities so that it may be possible to resolve them. This remains to be seen and the study of the MESA eigenfrequencies of such models could provide some clues as to their properties. This is left for a future investigation.

Finally, it is worth commenting on the limitations of this approach and future work. Non-radial modes are generally not observable in distant galaxies and so the specialisation to radial modes is sensible. We have only studied adiabatic oscillations, however, it is well-known that Cepheid pulsations are driven by non-adiabatic effects. Indeed, the blue edge of the instability strip corresponds to the location in the HR diagram where the motion becomes non-adiabatic inside the ionisation layer. This appears as a driving term in the LAWE and the generalisation to MG is straightforward. This driving mechanism depends only on atomic physics and thermodynamics, which are insensitive to MG and so the MG equivalent is simply the MLAW with exactly the same driving term. What is different is the internal structure of the star and it is entirely possible that the location of the blue edge is different in MG. Furthermore, with this driving term the MLAW is inhomogeneous and one can derive the amplitude as well as the frequency, and so

one could, in theory, derive the modified period-mass-luminosity (P-M-L) relation in MG without needing to perturb the GR calibrated one. This is left for future work, however, we remark that the driving term tends to excite the fundamental frequency, which is precisely what we have calculated here.

We have ignored the effects of scalar radiation, which is known to be negligible in chameleon-like theories, which have been the focus of this work. It is still unclear whether this is the case for Galileon-like theories and this too is left for a future investigation. It would also be interesting to see if effects that arise in coupled systems, such as beating patterns in the P-L relation, could be present, although this is beyond the scope of this work.

Here, we shall be content to present the theory and underlying framework for describing perturbations in modified gravity and to have shown that the full analytic treatment can lead to effects far stronger than one would naïvely expect given the modified equilibrium structure alone.

ACKNOWLEDGMENTS

I am incredibly grateful to Eugene Lim for several helpful discussions and suggestions. This work has greatly benefited from discussions with Avery Broderick, Phillip Chang and Bhuvnesh Jain. I am also thankful for conversations with Mustafa Amin, Anne-Christine Davis, Tom Hogan, Lam Hui, Will Keen, Levon Pogosian, Fabian Schmidt, Alessandra Silvestri and Vinu Vikram. I would like to thank the anonymous referee, whose questions and suggestions have greatly improved the quality of this paper. I am supported by the STFC.

Appendix A: Implementation of Modified Gravity into MESA

MESA [47, 48] is a publicly available program capable of solving the complete system of stellar structure equations coupled to the radiative transfer system, stellar atmosphere models, nuclear burning networks, convective motion and micro-physical processes such as opacity and electron degeneracy. It also includes effects such as overshooting, mass-loss and rotation in a fully consistent manner. Given some initial mass, it generates a pre-main-sequence stellar model and dynamically evolve it through the main-sequence and subsequent post-main-sequence to its final state, be it a white dwarf, neutron star or core-collapse supernova. Here, we are mainly interested in the main-sequence and post-main-sequence phases and so we shall limit our discussion to these.

MESA is a one-dimensional code (in that it assumes spherical symmetry) that divides the star into a series of variable-length cells, each with a specific set of quantities such as temperature, density, mass fraction etc. that may correspond to the values at either the cell centre

or boundary. Exactly which depends on the quantity in question, however it is always possible to interpolate between the two. We implement the effects of modified gravity by updating these assignments to include a cell-centred value of G , which differs from the Newtonian value in the region exterior to the screening radius. This implementation uses a quasi-static approximation where, given some initial radial profile, the star is evolved to its new equilibrium structure one time-step later. Using this profile, we integrate equation (12) to successively deeper cells until it is satisfied. The radius of this cell is then designated the screening radius and we then update the value of G in each cell according to equation (10) so that

$$G(r) = G \left[1 + \alpha \left(1 - \frac{M(r_s)}{M(r)} \right) \right] \quad r \geq r_s. \quad (\text{A1})$$

We then let the model evolve one time-step further to find the modified structure. This approximation is valid provided that the time-step between successive models is smaller than the time-scale on which changes to $G(r)$ are important and MESA provides a facility to ensure this is always the case. Furthermore, [25] have modified MESA for the same purpose of us using a scalar field ansatz and cell interpolation and we have verified that our results are indistinguishable from theirs.

This modified version of MESA was presented and studied in [26] and was used to make quantitative predictions of modified Cepheid pulsation frequencies in [27]. More details can be found in these references.

Appendix B: Numerical Techniques

Here we briefly describe the numerical methods used in order to obtain solutions of the MLawe. Whereas the form presented in equation (48) is useful for extracting the new physical features, numerically, it is more convenient to work with a first order system. One may re-write the homogeneous MLawe in the form

$$\frac{d}{dr} \left[\frac{\Gamma_{1,0} P_0}{r^2} \frac{d}{dr} (r^3 \xi) \right] - 4 \frac{dP_0}{dr} - 4\pi\alpha G \rho_0^2 r \xi + \omega^2 r \rho_0 \xi = 0. \quad (\text{B1})$$

In order to cast this into first order form we introduce the new variable η , defined by

$$\eta(r) = \frac{1}{r^2} \frac{d}{dr} (r^3 \xi), \quad (\text{B2})$$

which, using equation (34), is nothing but $-\delta\rho/\rho_0$. Using this definition, we can cast (B1) into a convenient first-order form for both Lane-Emden and MESA models.

1. Lane-Emden Form

When solving for Lane-Emden profile, we replace r with y using (78) and the pressure and density with θ

to obtain

$$\frac{d\eta}{dy} = \frac{1}{\Gamma_{1,0}\theta} \left[4(n+1) \frac{d\theta}{dy} \xi + \alpha(n+1)y\theta^n \xi \right. \quad (\text{B3})$$

$$\left. - (n+1)\Gamma_{1,0} \frac{d\theta}{dy} \eta - \tilde{\omega}^2 y \xi \right] \\ \frac{d\xi}{dy} = \frac{\eta - 3\xi}{y}, \quad (\text{B4})$$

where $\Gamma_{1,0}$ is treated as constant in Lane-Emden models, $\tilde{\omega}$ is defined in (85) and the term proportional to α is present only when $r > r_s$. The value of $\Gamma_{1,0}$ may be chosen at will. These are supplemented by the boundary conditions

$$\eta(0) = 3\xi(0) \quad (\text{B5})$$

$$\eta(y_R) = \frac{\xi(y_R)}{\Gamma_{1,0}} \left(4 + \frac{\tilde{\omega}^2 y_R}{(n+1) d\theta/dy} \right) \Big|_{y=y_R}, \quad (\text{B6})$$

which are the Lane-Emden equivalents of (53) and (54). We solve this equation using the shooting technique. Using the fourth-order Runge-Kutta method, we solve equations (B3) and (B4) in conjunction with the modified Lane-Emden equation (79) using a trial value of $\tilde{\omega}^2$ and the centre boundary condition (B5). We then test the surface condition (B6) against our solution, iterating over different values of $\tilde{\omega}^2$ until the difference between our solution and the boundary condition is less than some predefined tolerance (exactly how much depends on the accuracy required for the eigenvalue). Using this method, one can obtain $\tilde{\omega}^2$ and the corresponding eigenfunction to the desired accuracy.

2. MESA form

MESA produces pressure, density, temperature etc. profiles in physical units, and so it is convenient to use the

dimensionless quantities defined in (58), (59) and (60) so that the MLawe is

$$\frac{d\eta}{dx} = (\Gamma_{1,0}(x)\bar{P}_0(x))^{-1} \left[-\eta \left(\bar{P}_0 \frac{d\Gamma_{1,0}}{dx} + \Gamma_{1,0} \frac{d\bar{P}_0}{dx} \right) \right. \quad (\text{B7})$$

$$\left. + 4 \frac{d\bar{P}_0}{dx} + 4\pi\alpha x \bar{\rho}_0^2 \xi - \Omega^2 x \bar{\rho}_0 \xi \right], \quad (\text{B8})$$

$$\frac{d\xi}{dx} = \frac{\eta - 3\xi}{x}, \quad (\text{B9})$$

where, again, the term proportional to α is only present when $x > x_s \equiv r_s/R$ and Ω^2 is the dimensionless eigenfrequency defined in (63).

The eigenvalue problem is solved in a similar manner to the Lane-Emden models: using profiles for \bar{P}_0 and $\bar{\rho}_0$ at both the cell boundaries and centres as well as the screening radius for specified models from the modified version of MESA described in Appendix A these equations are integrated from the stellar centre using the fourth order Runge-Kutta scheme for a test value of Ω^2 . Ω^2 is then iterated until the boundary condition at the stellar surface,

$$\eta(1) = \frac{1}{\Gamma_{1,0}(1)} (\Omega^2 + 4) \xi(1), \quad (\text{B10})$$

is satisfied up to some pre-set tolerance. In this manner, Ω^2 and the corresponding eigenfunction can be found for any given model and the period found by inverting (63).

-
- [1] L. Amendola *et al.* (Euclid Theory Working Group), (2012), arXiv:1206.1225 [astro-ph.CO].
 - [2] Z. Ivezić, J. Tyson, R. Allsman, J. Andrew, and R. Angel (LSST Collaboration), (2008), arXiv:0805.2366 [astro-ph].
 - [3] T. Clifton, P. G. Ferreira, A. Padilla, and C. Skordis, Phys.Rept. **513**, 1 (2012), arXiv:1106.2476 [astro-ph.CO].
 - [4] S. Weinberg, Phys.Rev. **138**, B988 (1965).
 - [5] E. J. Copeland, M. Sami, and S. Tsujikawa, Int.J.Mod.Phys. **D15**, 1753 (2006), arXiv:hep-th/0603057 [hep-th].
 - [6] C. Will, Pramana **63**, 731 (2004).
 - [7] J. Khoury and A. Weltman, Phys.Rev.Lett. **93**, 171104 (2004), arXiv:astro-ph/0309300 [astro-ph].
 - [8] J. Khoury and A. Weltman, Phys. Rev. **D69**, 044026 (2004), arXiv:astro-ph/0309411.
 - [9] K. Hinterbichler and J. Khoury, Phys. Rev. Lett. **104**, 231301 (2010), arXiv:1001.4525 [hep-th].
 - [10] P. Brax, C. van de Bruck, A.-C. Davis, and D. Shaw, Phys. Rev. **D82**, 063519 (2010), arXiv:1005.3735 [astro-ph.CO].
 - [11] A. Vainshtein, Phys.Lett. **B39**, 393 (1972).
 - [12] A. Nicolis, R. Rattazzi, and E. Trincherini, Phys.Rev. **D79**, 064036 (2009), arXiv:0811.2197 [hep-th].
 - [13] E. Babichev, C. Deffayet, and R. Ziour, JHEP **0905**, 098 (2009), arXiv:0901.0393 [hep-th].
 - [14] K. Hinterbichler, Rev.Mod.Phys. **84**, 671 (2012), arXiv:1105.3735 [hep-th].
 - [15] T. S. Koivisto, D. F. Mota, and M. Zumalacarregui, Phys.Rev.Lett. **109**, 241102 (2012), arXiv:1205.3167 [astro-ph.CO].
 - [16] A. Barreira, B. Li, A. Sanchez, C. M. Baugh, and S. Pascoli, Phys.Rev. **D87**, 103511 (2013), arXiv:1302.6241

- [astro-ph.CO].
- [17] A. Barreira, B. Li, W. A. Hellwing, C. M. Baugh, and S. Pascoli, (2013), arXiv:1306.3219 [astro-ph.CO].
- [18] A. Barreira, B. Li, C. Baugh, and S. Pascoli, (2013), arXiv:1308.3699 [astro-ph.CO].
- [19] P. Brax, A.-C. Davis, B. Li, and H. A. Winther, (2012), arXiv:1203.4812 [astro-ph.CO].
- [20] J. Wang, L. Hui, and J. Khoury, (2012), arXiv:1208.4612 [astro-ph.CO].
- [21] W. Hu and I. Sawicki, Phys.Rev. **D76**, 064004 (2007), arXiv:0705.1158 [astro-ph].
- [22] B. Li, G.-B. Zhao, and K. Koyama, Mon.Not.Roy.Astron.Soc. **421**, 3481 (2012), arXiv:1111.2602 [astro-ph.CO].
- [23] P. Brax, A.-C. Davis, B. Li, H. A. Winther, and G.-B. Zhao, (2012), arXiv:1206.3568 [astro-ph.CO].
- [24] P. Brax, A.-C. Davis, B. Li, H. A. Winther, and G.-B. Zhao, JCAP **1304**, 029 (2013), arXiv:1303.0007 [astro-ph.CO].
- [25] P. Chang and L. Hui, (2010), arXiv:1011.4107 [astro-ph.CO].
- [26] A.-C. Davis, E. A. Lim, J. Sakstein, and D. Shaw, Phys.Rev. **D85**, 123006 (2012), arXiv:1102.5278 [astro-ph.CO].
- [27] B. Jain, V. Vikram, and J. Sakstein, (2012), arXiv:1204.6044 [astro-ph.CO].
- [28] L. Hui and A. Nicolis, Phys.Rev.Lett. **109**, 051304 (2012), arXiv:1201.1508 [astro-ph.CO].
- [29] B. Jain and J. VanderPlas, JCAP **1110**, 032 (2011), arXiv:1106.0065 [astro-ph.CO].
- [30] J. Lee, G.-B. Zhao, B. Li, and K. Koyama, (2012), arXiv:1204.6608 [astro-ph.CO].
- [31] V. Vikram, A. Cabre, B. Jain, and J. VanderPlas, (2013), arXiv:1303.0295 [astro-ph.CO].
- [32] A. Cabre, V. Vikram, G.-B. Zhao, B. Jain, and K. Koyama, JCAP **1207**, 034 (2012), arXiv:1204.6046 [astro-ph.CO].
- [33] Strictly speaking, this is not correct since $d\beta(\phi)/d\phi$ is a dimensionful quantity and should be compared with another physically relevant variable with the same dimensions. In the unscreened region the field is a small perturbation $\delta\phi$ about the background field value ϕ_0 such that $\delta\phi \ll \phi_0$. In this case one has $(d\beta/d\phi)\delta\phi \ll \beta(\phi_0)$. When deriving both the screening mechanism and the perturbation equations in modified gravity hydrodynamics the terms proportional to $d\beta/d\phi$ are always suppressed by factors of $\beta/\delta\phi$ relative to the other terms and so we will neglect them by setting $d\beta/d\phi$ to zero.
- [34] B. Jain and J. Khoury, Annals Phys. **325**, 1479 (2010), arXiv:1004.3294 [astro-ph.CO].
- [35] J. Khoury, (2010), arXiv:1011.5909 [astro-ph.CO].
- [36] P. Brax, (2012), arXiv:1211.5237 [hep-th].
- [37] One may wonder how accurate this approximation is. [25] have studied the effects of chameleon gravity on the structure an evolution of stars by solving the field equations numerically using a non-linear Gauss-Seidel solver. They have found that the approximation used here gives results very close to the full numerical solution and that any differences are negligible.
- [38] One must note however that this analysis applies to isolated objects only. In the presence of other objects of Newtonian potential Φ_N^{ext} the external potential can be large enough to screen an object that would otherwise be self-unscreened [40]. This environment dependence has formed the basis for many observational tests of these theories [26, 27, 29, 31, 32] and indeed the new effects presented here will rely on this feature as a potential probe.
- [39] P. Brax, C. van de Bruck, A.-C. Davis, and D. J. Shaw, Phys.Rev. **D78**, 104021 (2008), arXiv:0806.3415 [astro-ph].
- [40] L. Hui, A. Nicolis, and C. Stubbs, Phys.Rev. **D80**, 104002 (2009), arXiv:0905.2966 [astro-ph.CO].
- [41] F. Schmidt, M. V. Lima, H. Oyaizu, and W. Hu, Phys. Rev. **D79**, 083518 (2009), arXiv:0812.0545 [astro-ph].
- [42] P. Brax, A.-C. Davis, and J. Sakstein, Phys. Lett. B **719**, 210 (2013), arXiv:1212.4392 [hep-th].
- [43] P. Brax, A.-C. Davis, and J. Sakstein, (2013), arXiv:1302.3080 [astro-ph.CO].
- [44] HI gas clouds in galaxies have Newtonian potentials of order 10^{-11} [40], although, to-date, no observational tests exploiting this have been attempted.
- [45] W. L. Freedman and B. F. Madore, Ann.Rev.Astron.Astrophys. **48**, 673 (2010), arXiv:1004.1856 [astro-ph.CO].
- [46] There may be indirect changes due to the change in the structure of the fluid, for example the surface temperature, but these are not the direct result of a gravitational interaction but rather a response of the system to a change in the force [26].
- [47] B. Paxton *et al.*, Astrophys. J. Suppl. **192**, 3 (2011), arXiv:1009.1622 [astro-ph.SR].
- [48] B. Paxton, M. Cantiello, P. Arras, L. Bildsten, E. F. Brown, *et al.*, (2013), arXiv:1301.0319 [astro-ph.SR].
- [49] One could derive the full, fourth-order system of equations governing non-radial oscillations, however, its solutions are irrelevant for observational tests of modified gravity.
- [50] The sharp-eyed reader will notice that there is no term proportional to $d\beta/d\phi$ as one would expect. Technically, such a term should be present, however, we have already seen in section (II B) that this is negligible in theories of interest. In fact, it is a requirement of the screening mechanism that such derivatives are negligible and so we have set this term to zero when perturbing the momentum equation.
- [51] If this is not the case one can either canonically normalise if possible or define a more general form of $\beta(\phi)$ in terms of $C(\phi)$ and the field-dependent factor multiplying the kinetic term.
- [52] C. de Rham, G. Gabadadze, and A. J. Tolley, Phys.Rev.Lett. **106**, 231101 (2011), arXiv:1011.1232 [hep-th].
- [53] A. Silvestri, Phys.Rev.Lett. **106**, 251101 (2011), arXiv:1103.4013 [astro-ph.CO].
- [54] A. Upadhye and J. H. Steffen, (2013), arXiv:1306.6113 [astro-ph.CO].
- [55] Of course, we also need to derive the value of ω^2 from the solution of the equation. This can be done by looking for values such that the solutions satisfy both boundary conditions and is discussed in section (IV B).
- [56] J. Cox, *The Theory of Stellar Pulsation*, Princeton series in astrophysics (Princeton University Press, 1980).
- [57] Corrections from general relativity increase this critical value to $4/3 + \mathcal{O}(1)GM/R$ [73], where the $\mathcal{O}(1)$ factor depends on the specific composition of the star. We are interested in the properties of main-sequence stars with $GM/R \sim 10^{-6}$ and Cepheid stars with $GM/R \sim 10^{-7}$ –

- 10^{-8} and so this correction is always negligible compared with the effects of MG, which are of the same order as the non-relativistic contribution when the star is unscreened.
- [58] The reader may wonder why the star is more stable in MG when the stability criterion in GR does not change if one changes the value of G . When the star is unscreened we have $G \rightarrow G(1 + \alpha)$ and so one may expect any MG effects to vanish in this limit. In GR, there is an exact cancellation coming from the perturbations to the momentum equation (16) and the Newtonian potential. In MG, the additional gravitational force is not derived from the Newtonian potential but from the field profile and so any cancellation must come from the perturbation to the field equation. A priori, there is no reason why the field perturbations should cancel this new contribution and, indeed, we see here that they do not.
- [59] The reader should note that this is a varying function of χ_0 and so is not universal.
- [60] Conventionally, ξ is used to represent the Lane-Emden coordinate, however we have already used this for the radial perturbation and so here we use $y = r/r_c$ instead. This coordinate is identical to the one used in [26] when $n = 3$.
- [61] M. Hurley, P. H. Roberts, and K. Wright, *Astrophys. J.* **143**, 535 (1966).
- [62] This is not possible in the case $n = 3$ since there is no mass-radius relation. The absence of such a relation has the result that the constant K must vary as a function of stellar mass, χ_0 and α . For this reason, there is no meaningful way to compare perturbations of stars in MG since one is comparing stars with different equations of state. For this reason, we will not consider perturbations of these models.
- [63] R. Kippenhahn and A. Weigert, *Stellar structure and evolution*, Astronomy and astrophysics library (Springer, 1990).
- [64] Compared to the result that would be obtained if we had used a fully-unscreened profile. The equilibrium structure is still a small over-estimate of the effects of MG. For our purposes, this is not an issue since we seek only to investigate the new effects of MG oscillations and do not compare any of these results with real stars. When we analyse MESA predictions we will use a fully consistent approach.
- [65] I. Epstein, *Astrophys. J.* **112**, 6 (1950).
- [66] We have already argued in the previous subsection that the first case is highly unphysical and ambiguous. This is true if we wish to discern how the MG perturbations affect the numerical value of the oscillation periods but here we seek only to qualitatively investigate how the modified equilibrium structure influences the critical adiabatic index. Hence, for this purpose it is a reasonable case to investigate.
- [67] Some other pulsating objects such as RR Lyrae stars can be resolved in the local group but this is necessarily screened and so these objects cannot be used to probe MG. One requires an unscreened distance indicator at suitably large distances such that the dwarf galaxy is unscreened and there is another screened distance indicator which can be used in a comparison.
- [68] Y. Alibert, I. Baraffe, P. Hauschildt, and F. Alard, *Astron.Astrophys.* **344**, 551 (1999), arXiv:astro-ph/9901294 [astro-ph].
- [69] There is some ambiguity in the literature as to the precise definition of first-crossing. Here, we mean that the star has ascended the red-giant branch and subsequently looped, crossing the strip for the first time and not the brief, unobservable crossing after the main-sequence.
- [70] This is not to say that the approximation used by [27] is not applicable, rather that numerically calculating the period will give spurious results due to the lack of a suitable GR model to compute the unmodified period.
- [71] S. Hatton, J. E. Devriendt, S. Ninin, F. R. Bouchet, B. Guiderdoni, *et al.*, *Mon.Not.Roy.Astron.Soc.* **343**, 75 (2003), arXiv:astro-ph/0309186 [astro-ph].
- [72] J. Sakstein, A. Pipino, J. E. Devriendt, and R. Maiolino, *Mon.Not.Roy.Astron.Soc.* **410**, 2203 (2011), arXiv:1008.4158 [astro-ph.CO].
- [73] S. Chandrasekhar, *Phys.Rev.Lett.* **12**, 114 (1964).